UNIVERSITY OF OKLAHOMA

GRADUATE COLLEGE

STREAMSCOPE: FIXED-MOUNT LASER SCANNING INSTRUMENTATION FOR REMOTE STREAM GAUGING IN SHALLOW RIVERS WITH FREQUENTLY CHANGING GEOMORPHOLOGIES

A THESIS

SUBMITTED TO THE GRADUATE FACULTY

in partial fulfillment of the requirements for the

Degree of

MASTER OF SCIENCE

By

BRADEN JAMES WHITE
Norman, Oklahoma
2025

Downloaded from SHAREOK. Persistent Handle URL: https://hdl.handle.net/11244/341536

STREAMSCOPE: FIXED-MOUNT LASER SCANNING INSTRUMENTATION FOR REMOTE STREAM GAUGING IN SHALLOW RIVERS WITH FREQUENTLY CHANGING GEOMORPHOLOGIES

A THESIS APPROVED FOR THE
SCHOOL OF ELECTRICAL AND COMPUTER ENGINEERING

BY THE COMMITTEE CONSISTING OF

Dr. Hjalti Sigmarsson, Chair

Dr. Golnaz Habibi

Dr. Pierre Kirstetter

© Copyright by BRADEN JAMES WHITE 2025
All Rights Reserved.

Acknowledgements

I would like to extend my deepest gratitude to Dr. Jonathan Gourley and Dr. Jorge Duarte for their unwavering support throughout the development of StreamScope. From early morning trips to Falls Creek to patiently reading through my late-night epiphanies—often delivered as walls of text sent at questionable hours—their guidance, patience, and insight have been invaluable. Their dedication made this project not only possible, but deeply fulfilling. I could not have asked for better mentors.

I am also sincerely thankful to Danny Wasielewski for his thoughtful input and practical advice throughout the design process. Even when certain approaches seemed unworkable, his perspective helped steer the project toward effective and achievable solutions.

My thanks go as well to the United States Geological Survey for placing their trust in me. Being given the freedom and responsibility to independently design StreamScope from the ground up was an extraordinary opportunity—one that few engineers get to experience. That trust has profoundly shaped me into a more capable and confident engineer.

I am eternally grateful to my mentors and friends in Sooner Competitive Robotics. Much of my design intuition and many of the interdisciplinary skills I brought to this project were developed during my time in SCR. Without that experience, I would not have had the confidence or ability to take on a project of this scope and complexity.

I also want to thank my friend Luis Ferrari. Even from miles away, he was a steady source of motivation and support. Our regular phone calls gave me a space to reflect, recharge, and stay focused throughout the process. His friendship and encouragement meant a great deal, and I'm truly grateful for his presence every step of the way.

Finally, I want to thank my family—my mom, dad, and sister—for their constant love and support. Their belief in me and encouragement throughout my life have meant more than words can express. Their support fills every step of my journey.

Table of Contents

Acknowledgements **iv**

List Of Tables **viii**

List Of Figures **ix**

Abstract **xi**

1 Introduction **1**
1.1 Overview . . . 1
1.2 Existing Approaches to Surveying Stream Bathymetry . . . 2
1.2.1 Total Station Survey . . . 2
1.2.2 Airborne Bathymetric LiDAR . . . 4
1.2.3 Photogrammetry Survey . . . 6
1.2.4 Pros and Cons of Existing Approaches . . . 8
1.3 Project Motivation . . . 8
1.4 Thesis Outline . . . 10

2 StreamScope: A Fixed-Mount Laser Scanning Instrument for Real-Time Stream Monitoring **12**
2.1 System Concept . . . 12
2.2 Assumed Advantages Over Existing Approaches . . . 13
2.3 Fundamental Requirements . . . 14
2.3.1 USGS Requirements . . . 14
2.3.2 Functional Requirements . . . 15

3 StreamScope Development **18**
3.1 Overview . . . 18
3.2 Peripheral Selection . . . 18
3.2.1 Laser Distance Module . . . 18
3.2.2 Sonar Tank Sensor . . . 19
3.2.3 Inclinometer . . . 20
3.2.4 Servo Motor . . . 21
3.2.5 Microcontroller . . . 22

3.3 Mechanical Design and Assembly . . . 23
3.3.1 Scanning Module and Enclosure Design . . . 23
3.3.2 Mounting Configuration . . . 28
3.4 Printed Circuit Board Design . . . 29
3.4.1 Power Distribution Board . . . 30
3.4.2 Control Board . . . 32
3.5 Firmware . . . 35
3.5.1 Modbus RS-485 Communication . . . 35
3.5.2 Scanning Pipeline . . . 36
3.5.2.1 Initialization . . . 36
3.5.2.2 Polling Modbus . . . 39
3.5.2.3 Conducting a Sweep . . . 40
3.5.2.4 Processing Measurements . . . 43
3.5.2.5 SD Card Logging . . . 44
3.5.3 Safeguards and Fail-Safes . . . 45
3.6 Data Post-Processing . . . 46
3.6.1 Centroid Estimation Using 2D Kernel Density Estimation . . . 47
3.6.2 Locating the Left and Right Bank Coordinates . . . 51
3.6.3 Pruning Consistent, Erroneous Measurements . . . 51
3.6.4 Cross-Sectional Area Calculation . . . 52

4 Laboratory Experiments **54**
4.1 Overview . . . 54
4.2 Laser Performance Under Ambient Solar Radiation Conditions . . . 55
4.2.1 Background . . . 55
4.2.2 Methodology . . . 55
4.2.3 Results . . . 57
4.2.4 Conclusions . . . 59
4.3 Laser Performance Under Increasing Turbidity . . . 60
4.3.1 Background . . . 60
4.3.2 Methodology . . . 60
4.3.2.1 Height Experiment . . . 62
4.3.3 Results . . . 64
4.3.3.1 Bottom Substrate - Sand . . . 65
4.3.3.2 Bottom Substrate - Rock . . . 72
4.3.3.3 Height Increase . . . 73
4.3.4 Discussion . . . 74
4.4 Accelerometer Accuracy for Angle Calculation . . . 80
4.4.1 Background . . . 80
4.4.2 Methodology . . . 80
4.4.3 Results . . . 81

4.4.4 Conclusion 81

5 Field Deployment **82**
5.1 Overview 82
5.2 Description of Setting 83
5.3 Deployment Configuration 85
5.4 Scanning Setup and Strategy 88
5.5 Retrieval of Cross-Sections 89
5.6 Comparison to Total Station Survey Conducted by the United States Geological Survey 93

6 Conclusions **97**
6.1 Summary of Work 97
6.2 Contributions 98
6.3 Future Work 99
6.3.1 Enhanced Laser Range Finder with Signal Access 99
6.3.2 Self-Sufficient StreamScope 100
6.3.3 Adaptive Post-Processing Techniques 101

List Of Tables

1.1 Pros and Cons of Bathymetric Survey Techniques 8

2.1 Mapped USGS Requirements and Corresponding Functional Requirements 15

4.1 Results from Solar Radiation Experiment - Table 58
4.2 Turbidity Experiment Table - 120 mm Depth (Sand Bottom) 65
4.3 Turbidity Experiment Table - 150mm Depth (Sand Bottom) 66
4.4 Turbidity Experiment Table - 200mm Depth (Sand Bottom) 67
4.5 Turbidity Experiment Table - 250mm Depth (Sand Bottom) 68
4.6 Turbidity Experiment Table - 300mm Depth (Sand Bottom) 69
4.7 Turbidity Experiment Table - 350mm Depth (Sand Bottom) 70
4.8 Turbidity Experiment Table - 400mm Depth (Sand Bottom) 71
4.9 Turbidity Experiment Table - 350mm Depth (Rock Bottom) 72
4.10 Turbidity Experiment Table - 350mm Depth (Sand, Height Increase) . 73

List Of Figures

1.1 Total Station Instrument 2
1.2 USGS Total Station Survey at Falls Creek in Davis, OK (Oct 2024) . . 3
1.3 Water Absorption Coefficient of Different Wavelengths 5
1.4 EAARL LiDAR [5] 6
1.5 Adjusting for Refraction Utilizing Photogrammetry [4] 7

2.1 Snell's Law-based distance correction for laser measurements intersecting a stream's surface. d_{measured}: measured distance returned by the laser; θ_{air}: angle of incidence of the laser beam in air; h_{sonar}: vertical distance from the sonar to the water surface; n_{air}: refractive index of air (1.00029); n_{water}: refractive index of water (1.333); x, y: corrected Cartesian coordinates of the measurement point relative to the sensor. . 13

3.1 Egismos Laser Distance Module (Version 2) [7] 19
3.2 MaxBotix MB7388 HRXL-MaxSonar-WRMLT [8] 20
3.3 Adafruit ADXL343 - Triple-Axis Accelerometer [9] 21
3.4 Tilt Angle Calculation from Accelerometer Data 21
3.5 HiTec D646WP Waterproof Servo [12] 22
3.6 Teensy 4.1 Microcontroller [11] 23
3.7 Initial StreamScope Design 24
3.8 Scanning Module CAD 25
3.9 Scanning Module 25
3.10 Scanning Module After A Rainstorm 26
3.11 Servo Attachment 27
3.12 Top-Down View of StreamScope 28
3.13 StreamScope Mounting Configuration 29
3.14 Power Distribution Schematic (7V Buck Converter) 30
3.15 Power Distribution Schematic (Outputs) 31
3.16 Power Distribution 3D Model 32
3.17 Control Board Schematic (Page 1) 33
3.18 Control Board Schematic (Page 2) 34
3.19 Control Board 3D Model 34
3.20 Sample of Modbus Registers Used for StreamScope 36
3.21 Variable Clock Speed Routine for the Teensy 4.1 38
3.22 Conditional Statement for a General Sweep 40
3.23 Low Pass Filter for Angular Feedback 42
3.24 Calculating Coordinate Points Using Snell's Law 44
3.25 StreamScope Log File 44
3.26 Return Differences at the Same Angle Over Multiple Consecutive Sweeps 48

3.27 2D Kernel Density Estimation With a Gaussian Kernel 48
3.28 Uncertain Centroids Filling the Gap Around 0° for a Cross-Section . . . 50
3.29 Gauss's Area Formula for Irregular Polygons 53

4.1 Solar Radiation Experiment Setup 56
4.2 Verifying Water Height With Tape Measure 57
4.3 Results from Solar Radiation Experiment - Graph 58
4.4 Turbidity Experiment Setup 61
4.5 Laser and EXO Sonde Set-Up For Turbidity Experiment 62
4.6 Height Increase Turbidity Experiment Setup - Side View 63
4.7 Height Increase Turbidity Experiment Setup - Upward View 63
4.8 Turbidity Experiment Graph - 120 mm Depth (Sand Bottom) 65
4.9 Turbidity Experiment Graph - 150mm Depth (Sand Bottom) 66
4.10 Turbidity Experiment Graph - 200mm Depth (Sand Bottom) 67
4.11 Turbidity Experiment Graph - 250mm Depth (Sand Bottom) 68
4.12 Turbidity Experiment Graph - 300mm Depth (Sand Bottom) 69
4.13 Turbidity Experiment Graph - 350mm Depth (Sand Bottom) 70
4.14 Turbidity Experiment Graph - 400mm Depth (Sand Bottom) 71
4.15 Turbidity Experiment Graph - 350mm Depth (Rock Bottom) 72
4.16 Turbidity Experiment Graph - 350mm Depth (Sand, Height Increase) . 73
4.17 Turbid Water During Turbidity Experiments 76
4.18 Egismos Scanning Through Turbid Water 78
4.19 Single Measurement vs Continuous Measurement Mode 79
4.20 Error Between Calculated Angle and Accelerometer Angle 81

5.1 Falls Creek - Davis, OK 83
5.2 Panoramic View of Falls Creek near Davis, OK 84
5.3 Deployment Scheme Diagram 85
5.4 Enclosures and Solar Panel at Falls Creek near Davis, OK 86
5.5 StreamScope Deployment Script Sending Data to Remote Server 87
5.6 StreamScope Deployed at Falls Creek near Davis, OK 87
5.7 Laser Beam Path During a Sweep 89
5.8 Erroneous Returns Early in Deployment 90
5.9 Turbulent Water at Falls Creek near Davis, OK 91
5.10 StreamScope Cross-Sections (05/14 - 05/19) 92
5.11 USGS Total Station Survey at Falls Creek near Davis, OK 94
5.12 StreamScope Cross-Section Compared to the USGS Cross-Section . . . 95

6.1 Prototype Green Laser Range Finder 99

Abstract

Accurate streamflow monitoring in shallow rivers with frequently changing geomorphology poses a unique challenge, particularly in remote and ungauged locations. This thesis presents a novel approach developed in collaboration with the United States Geological Survey (USGS) to generate real-time discharge estimates using a low-power, non-contact sensor system. StreamScope integrates a Class II 620 nm laser rangefinder with an ultrasonic sensor to remotely measure river cross-sectional geometry and develop stage–area ratings. Through onboard automation, the system captures high-resolution bathymetric data, enabling continuous discharge estimation without physical contact with the stream.

Laboratory experiments were conducted to evaluate the selected laser rangefinder under varying conditions of solar radiation, water turbidity, water depth, bottom substrate, and sensor height. The results demonstrated that the unit operates best under low solar radiation, is capable of obtaining measurements under low turbidity up to 20 NTU, and that the laser's returns may serve as a proxy for turbidity. Additionally, the tests established the operational limits of the sensor. The field deployment at Falls Creek in Davis, Oklahoma, demonstrated the robustness and precision of the instrument in a dynamic, real-world environment. The data collected provided a significant improvement in resolution compared to a traditional USGS stream survey.

Chapter 1

Introduction

1.1 Overview

Monitoring rivers with shallow depths and rapidly changing geomorphologies presents a significant challenge, particularly in remote and ungauged locations. In such environments, the relationships between water level, cross-sectional area, and flow rate are often inconsistent and highly variable over time, resulting in unreliable discharge data. This problem is especially acute in dynamic settings such as sandy-bed rivers, post-wildfire watersheds, and mountainous terrain. Limited physical access, safety risks, and the high costs associated with manual or airborne surveys further complicate data collection.

A cost-effective, real-time monitoring solution for these undersurveyed rivers could substantially improve hydrologic modeling, enhance flood forecasting, and provide timely insights into evolving stream conditions. The ideal system would be low-cost, low-power, easily deployable, and capable of continuous, autonomous operation.

Before introducing such a system, it is important to assess existing methods for retrieving channel bathymetry, along with their respective strengths and limitations. This context helps to underscore both the critical role of accurate stream measurements and the pressing need for more efficient alternatives—especially in environments with shallow water and dynamic geomorphologies.

1.2 Existing Approaches to Surveying Stream Bathymetry

1.2.1 Total Station Survey

The United States Geological Survey (USGS), which is responsible for surveying the vast majority of streams in the United States, utilizes an instrument manufactured by Trimble Geospatial called a Total Station to measure stream cross-sections and water surface elevations. A Total Station combines electronic distance measurement via laser range finder and angular measurements using an absolute encoder to determine the precise coordinates that make up the surveyed stream [1]. These coordinates can then be used to generate the stream's cross-section.



Figure 1.1: Total Station Instrument

The Total Station determines range using a time-of-flight (ToF) method, in which a 1550 nm infrared laser pulse is emitted and the time taken for the light to reflect off of the prism or reflective target and return to the sensor is measured [1].

The angular measurements are deduced by the Total Station's absolute encoders, which provides the exact angular position of the instrument without needing an initial reference or "zero" orientation [1].

During a stream cross-section survey, the Total Station is set up on stable ground near the stream channel. Before taking measurements, surveyors look through its optical scope to make sure that the Total Station is centered over its benchmark before beginning measurements. A survey rod with a prism or reflective target is placed manually at various points in the stream by a surveyor from one bank to another - often at regular intervals or locations where notable streambed elevation changes are observed [2]. These point measurements yield highly accurate data suitable for deriving the cross-sectional profile of the stream.



Figure 1.2: USGS Total Station Survey at Falls Creek in Davis, OK (Oct 2024)

Despite the Total Station survey being a source of reliable data, it is also time-consuming, labor-intensive, and expensive. A standard cross-sectional survey involves wading through streams and manually acquiring each discrete point in the channel. The total number of data points collected is constrained by the time allotted for the survey and the personnel available. Furthermore, these surveys are typically conducted infrequently, meaning they capture only snapshots in time and may miss critical changes during dynamic flow events such as floods or post-wildfire sediment transport. Because this methodology requires physical site access, clear weather, and line-of-sight, they are also impractical for high-frequency monitoring or deployment in remote, rugged, or hazardous terrains where access is limited or dangerous. Total Station instruments typically retail for thousands of dollars (USD) as well, making it impractical for routine surveys of small streams.

1.2.2 Airborne Bathymetric LiDAR

Airborne bathymetric Light Detection And Ranging (LiDAR) systems are commonly used to survey coastal areas and shallow bodies of water. The USGS Experimental Advanced Airborne Research LiDAR (EAARL) is an example of one of these instruments. EAARL uses a laser that operates in the green region of the electromagnetic spectrum around 532 nm because it is less attenuated than near-infrared lasers through water, which results in more favorable results compared to near-infrared light [3]. This can be seen in Fig. 1.4, where blue-green light is seen to have the lowest absorption coefficient through water when compared to other visible wavelengths.

Environmental conditions can significantly influence LiDAR returns. Several factors can influence the signal:

- Water surface turbulence (waves)

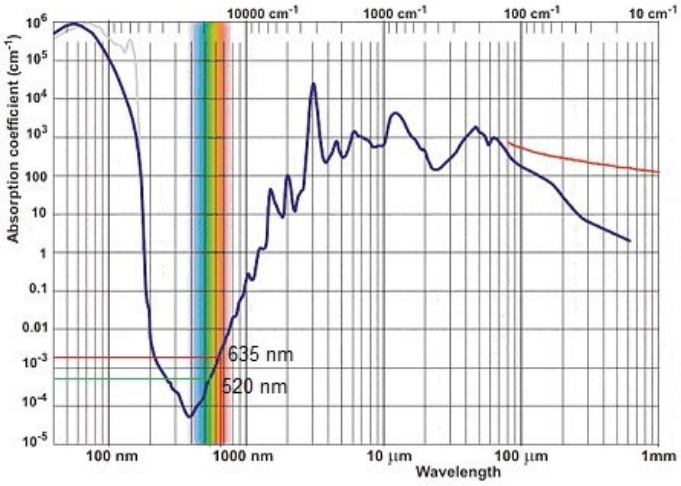

Figure 1.3: Water Absorption Coefficient of Different Wavelengths

- Aeration
- Bottom Substrate
- Turbidity, or how "murky" the water is depending on suspended sediment and organic matter [3].

Geolocation of the returns is accomplished using two GPS receivers and an IMU, which provide the position and orientation of the airborne platform during operation [3]. After a scan is conducted, the data is then subsequently processed using The Airborne Lidar Processing System (ALPS) which allows users to view information about the scan and utilize post-processing algorithms to produce bathymetric and topographic information [3].

Ultimately, airborne bathymetric LiDAR becomes impractical for use cases outside of coastal watersheds and large rivers. Green-blue LiDAR systems are highly specialized and expensive, making them inaccessible to most high-frequency monitoring efforts, unless created in-house. In addition, operational complexity such as flight planning, navigation, and data processing requires trained personnel [3]. This limits the

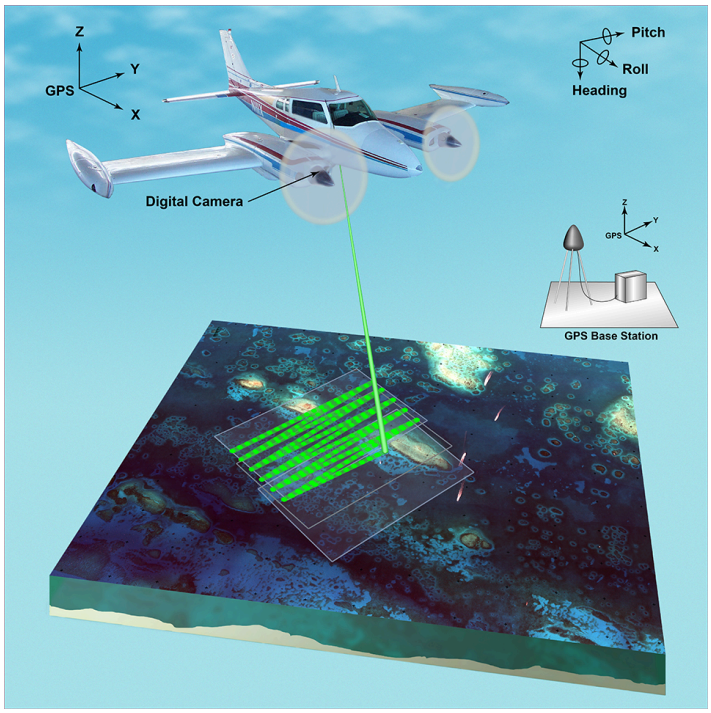

Figure 1.4: EAARL LiDAR [5]

feasibility of frequent data collection, particularly in logistically challenging environments. Even if the conditions and environment are optimal, airborne LiDAR captures only static snapshots of the changes that occur. Rapid changes in geometry are unable to be observed, as flights need to be coordinated in advance. Furthermore, laser classification presents another constraint: for any unattended system deployed over streams accessible to the public, the use of eye-safe lasers is essential to ensure safety and regulatory compliance.

1.2.3 Photogrammetry Survey

Photogrammetry is a method for deriving three-dimensional models from overlapping two-dimensional photographs using structure-from-motion techniques. By taking photos of the desired water feature from different angles, the prominent features present in both images can be matched to reconstruct the geometry of the scene [4]. When

water is present, these models must be corrected for refraction at the water surface using Snell's Law, as light bends when transitioning between air and water [4]. Once corrected, bathymetric data can be extracted from the resulting point cloud [4].

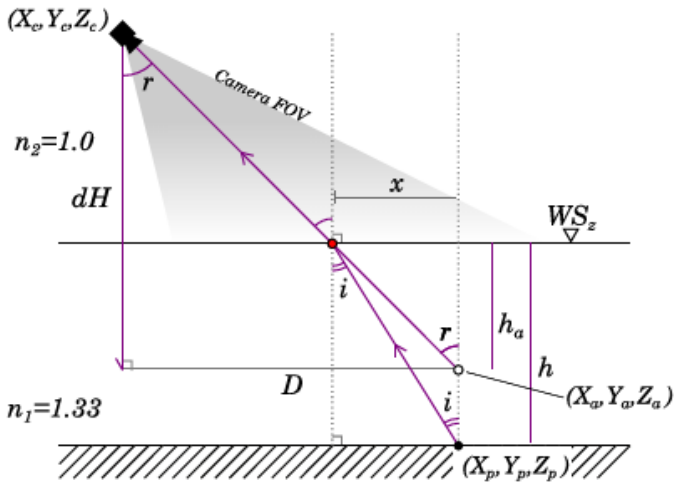

Figure 1.5: Adjusting for Refraction Utilizing Photogrammetry [4]

Photogrammetry faces significant limitations when applied to real-time or in-stream monitoring. The presence of flowing water introduces blur and reflective surfaces that interfere with the ability to accurately reconstruct the bathymetry [4]. Lighting conditions must be favorable to avoid shadows or overexposure. Additionally, photogrammetry depends on post-processing and ground control points for spatial accuracy, it is not conducive to unattended, continuous monitoring. The digital image processing required for reconstruction is computationally expensive, requiring additional tooling and computational power.

1.2.4 Pros and Cons of Existing Approaches

Technique	Pros	Cons
Total Station	• High accuracy • Minimal post-processing required	• Only captures singular points in time, suboptimal for continuous monitoring • High cost • Requires manual operation and trained personnel • Low precision, limited by time and personnel
Airborne Bathymetric LiDAR	• Rapid coverage of large areas • Simultaneous land and water mapping	• Only captures singular points in time, suboptimal for continuous monitoring • High cost • Requires manual operation and trained personnel • Unable to capture bathymetry of obstructed streams or granular data of smaller streams • Utilizes a laser that is not eye safe, preventing unattended operation.
Photogrammetry	• Inexpensive • Ability to collect data autonomously • If it utilizes a UAS, provides potential for retrieving multiple cross-sections along the channel	• Shadows affect measurements • Water needs to be clear, calm, and shallow • Post-processing is computationally expensive

Table 1.1: Pros and Cons of Bathymetric Survey Techniques

1.3 Project Motivation

Monitoring dynamic stream bathymetry requires precise, high-resolution, and temporally dense data collection. Methods such as Total Station surveys, airborne bathymetric LiDAR (e.g., the USGS EAARL system), and structure-from-motion photogrammetry have each contributed substantially to hydrologic research and are sufficient options for specific applications. However, each method comes with its own inherent

limitations that make them suboptimal for surveying rivers and streams in situations where:

- Conditions such as water level, sediment deposition and scour rapidly change
- Frequent and autonomous monitoring is desired
- The location is difficult to survey manually, such as mountainous or forested areas

To overcome these limitations, this thesis introduces StreamScope, a low-cost, low-power laser scanning instrument designed for autonomous and continuous operation. StreamScope is deployed in a fixed position—whether by cable, bridge, or other supports—to capture high-resolution, repeatable scans of the streambed, banks, and water surface. Its overhead deployment allows persistent monitoring without requiring human presence in the field, and its fixed spatial position ensures precise alignment between repeated measurements, enabling the detection of subtle morphological changes over time.

StreamScope addresses a key gap in current surveying capabilities by enabling high-temporal-resolution data collection in shallow and dynamic stream environments that are poorly served by existing technologies. Its compact form factor and energy-efficient design allow for long-term, solar-powered deployments, making it especially well suited for remote or difficult-to-access sites. By continuously monitoring processes such as sediment transport, erosion, and stage fluctuations, StreamScope provides a new and practical approach to observing channel dynamics in real time.

1.4 Thesis Outline

Chapter 2 introduces StreamScope, a fixed-mount laser scanning instrument designed for real-time stream monitoring of shallow streams with frequently changing geomorphologies. The chapter begins by outlining the system concept, explaining how StreamScope is intended to capture stream cross-sections and nearby features in a continuous, automated manner. This concept is contrasted with traditional monitoring methods, highlighting the expected improvements in data resolution, temporal frequency, and operational efficiency. The chapter then explores the assumed advantages of the StreamScope over the discussed existing approaches. Following this, the chapter defines the fundamental requirements for the system to operate as needed. It presents both externally imposed requirements, such as those established by the USGS and the general technical requirements derived from them. This chapter sets the stage for the technical design choices described in the following chapters by framing the system's intended role and the criteria it must meet to accomplish its goals.

Chapter 3 covers the development of the StreamScope system, starting with the selection of key components like the laser distance module, sonar, inclinometer, servo motor, and microcontroller and discusses the reasoning behind each choice. The chapter then details the mechanical aspect of the design, including the scanning mechanism, enclosure, and waterproofing considerations. The printed circuit board designs for the main control board and power distribution board are then examined in detail. Firmware aspects such as Modbus RS-485 communication, scanning control, data logging configuration, and fail-safes are described next. Finally, data post-processing techniques are discussed, including coordinate transformation, noise filtering with clustering, centroid analysis under varying conditions, and calculation of cross-sectional area.

Chapter 4 presents laboratory experiments conducted to evaluate the StreamScope system. It begins with tests of laser performance under ambient solar radiation conditions and discusses the effect on its returns. Next, the chapter examines laser performance as the turbidity increases, considering different bottom substrates such as sand and rock, changes in water depth and unit height, and disturbed water conditions. Finally, it assesses the accuracy of the accelerometer for accurately measuring the unit's roll angles.

Chapter 5 details the field deployment of the StreamScope system. It starts with an overview and describes the physical setting of the deployment at Falls Creek near Davis, Oklahoma. The chapter then explains the deployment configuration and scanning strategy used in the field. It covers how cross-sectional data was retrieved and concludes with a comparison of the StreamScope measurements to a Total Station survey conducted by the USGS and a subsequent manual survey, highlighting the system's accuracy and reliability in real-world conditions.

Chapter 6 concludes the thesis by summarizing the work presented throughout. It outlines the main contributions of the research and discusses potential avenues for future work to enhance and expand the StreamScope system.

Chapter 2

StreamScope: A Fixed-Mount Laser Scanning Instrument for Real-Time Stream Monitoring

2.1 System Concept

The system centers around a Class II pinpoint laser rangefinder mounted facing downwards on a vertically oriented servo motor. To initiate a scan, a user or script on the selected datalogger can specify deployment-specific parameters, including the number of angular increments and the number of distance measurements per angle. An angular feedback sensor is integrated to measure the laser's orientation throughout each sweep, ensuring accurate angular registration regardless of the unit's roll relative to the water surface.

The unit also includes a downward-facing ultrasonic rangefinder to directly measure the vertical distance to the water surface beneath the instrument. This water surface elevation data is essential for applying Snell's Law, allowing for refraction correction of laser distance retrievals that penetrate the water column. The methodology for this correction is described in Figure 2.1. For this correction to be applied effectively, the laser rangefinder must either provide access to the raw return signal or output unprocessed distance measurements. This correction not only improves the localization accuracy of submerged points but also facilitates water surface detection, enabling identification of channel banks and removal of erroneous laser returns.

$$\textbf{Given:} \quad d_{\text{measured}},\ \theta_{\text{air}},\ h_{\text{sonar}},\ n_{\text{air}} = 1.00029,\ n_{\text{water}} = 1.333$$

$$d_{\text{air}} = \frac{h_{\text{sonar}}}{\cos(\theta_{\text{air}})}, \quad d_{\text{water}} = d_{\text{measured}} - d_{\text{air}}$$

$$\textbf{If } d_{\text{water}} \leq 0: \quad x = \sin(\theta_{\text{air}}) \cdot d_{\text{measured}}, \quad y = \cos(\theta_{\text{air}}) \cdot d_{\text{measured}}$$

$$\textbf{Else:} \quad \theta_{\text{water}} = \sin^{-1}\left(\frac{n_{\text{air}}}{n_{\text{water}}} \cdot \sin(\theta_{\text{air}})\right)$$

$$x = \sin(\theta_{\text{air}}) \cdot d_{\text{air}} + \frac{\sin(\theta_{\text{water}})}{n_{\text{water}}} \cdot d_{\text{water}}, \quad y = h_{\text{sonar}} + \frac{\cos(\theta_{\text{water}})}{n_{\text{water}}} \cdot d_{\text{water}}$$

Figure 2.1: Snell's Law-based distance correction for laser measurements intersecting a stream's surface. d_{measured}: measured distance returned by the laser; θ_{air}: angle of incidence of the laser beam in air; h_{sonar}: vertical distance from the sonar to the water surface; n_{air}: refractive index of air (1.00029); n_{water}: refractive index of water (1.333); x, y: corrected Cartesian coordinates of the measurement point relative to the sensor.

Upon completion of a scan, the angle-distance pairs are post-processed into Cartesian coordinates. For each point, Snell's Law is applied when the calculated vertical coordinate is less than the measured sonar water surface height, indicating a submerged return. Following transformation, outliers are filtered out, and point centroids are identified at each angular increment. Points above the water surface are omitted from further analysis, and the cross-sectional area is computed based on the remaining submerged geometry.

2.2 Assumed Advantages Over Existing Approaches

StreamScope provides high-angular-resolution bathymetric measurements at consistent temporal intervals, overcoming the limitations of manual surveys, photogrammetry, and

airborne LiDAR. Its non-contact operation, low power consumption, and ease of deployment make it particularly suited for remote or dynamic environments. The system enables near-continuous observation of fluvial processes, including sediment transport, flash flooding, and post-wildfire hydrologic response, representing a significant step forward in scalable, real-time river monitoring.

2.3 Fundamental Requirements

Before discussing the development of StreamScope, it is important to outline the requirements that were set forth by the United States Geological Survey, as they provide context for the functional requirements and their corresponding design choices.

2.3.1 USGS Requirements

The USGS outlined the following, baseline requirements:

- **Operationalize a fixed-mount, laser scanning instrument capable of measuring cross-sectional geometry that is relatively low-cost and low-power.**
    - The unit will be deployed in remote areas, powered mainly by solar panels, so it needs to be relatively low-power so that it does not drain batteries faster than they can charge.
    - If the laser is rated higher than Class II—defined as a visible laser with power output up to 1 milliwatt—it poses a fire or eye hazard when operated unsupervised. Therefore, the chosen sensor must be Class II or lower.
- **Design the unit so that it is easy to replicate, utilizing readily available parts.**

- **Integrate measurements into USGS workflows and software to telemeter cross-sectional geometry data and produce real-time, stage-area ratings remotely.**

    - The USGS primarily uses dataloggers and sensors that use SDI-12, a single-wire serial protocol mainly used for environmental sensors with simple data returns, or Modbus over RS-485, an industrial communication protocol that uses 16-bit registers and a client/server system for exchanging data.
    - For remote deployment, sites are usually equipped with a dedicated data-logger, modem, solar panel, and 12V batteries. The data-logger could be a typical datalogger like the Sutron Satlink3 Logger/Transmitter or a Raspberry Pi.

2.3.2 Functional Requirements

Given the baseline requirements by the USGS, the scanning methodology, and context of operation, the functional requirements can be established:

Table 2.1: Mapped USGS Requirements and Corresponding Functional Requirements

USGS Requirements	**Functional Requirements**
Operationalize a fixed-mount, laser scanning instrument for measuring cross-sectional geometry	Must include a fixed, waterproof housing with an integrated laser sensor capable of high-resolution scanning in a configurable horizontal sweep across a channel

USGS Requirements	**Functional Requirements**
Low-cost for prototyping and scalable manufacturing	System total cost should remain below $1,000 per unit using off-the-shelf components and 3D-printed parts where applicable
Low-power for solar-based remote operation	Power consumption should be minimized where possible and measures to conserve power should be utilized in both hardware and firmware. Laser must be a Class II to ensure safe, unsupervised operation.
Electrical and software should be easy to understand and assemble	Printed circuit boards should be hand-solderable and the software should use easy-to-grasp languages and frameworks.
Simple, waterproof, easily reproducible enclosure	Enclosure should ideally be built based off an existing enclosure. Large modifications to the enclosure should be kept to a minimum to simplify the creation and limit failure points. Add-ons that are 3D printed should be printed using filament that is resistant to harsh outdoor conditions and coated to ensure it is waterproof.
Use of readily available sensors	Sensors should be easily obtainable from major suppliers. Ideally, these sensors should have plentiful, public documentation online.

USGS Requirements	**Functional Requirements**
Minimal specialized tooling required	With the exception of 3D-printed parts and enclosure holes, the unit should be able to be put together using inexpensive and accessible hand tools
Integrate into USGS workflows	Provide interfaces to format the data into formats that the USGS typically works with.
Support SDI-12 or Modbus protocols	System must support data transmission via either SDI-12 or Modbus RTU over RS-485 with configurable address and register mappings
Compatible with standard USGS site equipment (e.g., data loggers, solar panels, 12V batteries)	Must operate reliably from 12V DC with voltage tolerance of $\pm 10\%$, and output data compatible with Sutron Satlink3 or Raspberry Pi interfaces

Chapter 3

StreamScope Development

3.1 Overview

This chapter discusses the development of the StreamScope and the reasoning behind its sensor selection, enclosure and scanning mechanism design, electrical hardware and firmware design, and its post-processing pipeline.

3.2 Peripheral Selection

3.2.1 Laser Distance Module

Based on the requirements outlined in Table 2.1, the Egismos Laser Distance Module was selected for its compact size, minimal post-processing, Universal Asynchronous Receiver/Transmitter (UART) communication interface, and Class II laser classification. Its small footprint makes it ideal for integration into a custom mount designed to move the module bank-to-bank via a servo. The module supports multiple modes, including continuous and single-shot measurement.

The module utilizes a red laser between the 620-690 nm range. As mentioned in Section 1.2.2 when discussing airborne bathymetric LiDAR systems, lasers in the blue-green spectrum are typically used in bathymetric applications because of their lower absorption rate compared to other wavelengths. But, blue-green laser range finders



Figure 3.1: Egismos Laser Distance Module (Version 2) [7]

and LiDAR systems are rare and highly specialized, while red laser range finders are plentiful and sufficient for StreamScope's shallow water application. This will be shown in Chapter 4 through the laboratory experiments.

The module has a rated range of 100 meters, a rated accuracy of +/- 3 millimeters, and minimal post-processing, which is important as it allows for in-house post-processing to yield accurate results [7].

3.2.2 Sonar Tank Sensor

The MaxBotix MB7388 HRXL-MaxSonar-WRMLT was chosen for its high measurement resolution of 1 mm, low-power average current consumption of just 2.9 mA, and waterproof design [8]. It also contains redundancy for measuring the distance output, with both a UART and analog interface. Measurements can be read continuously as the sonar is connected to power, allowing for StreamScope to take measurements quickly and efficiently, without having to prompt the sensor for measurements.



Figure 3.2: MaxBotix MB7388 HRXL-MaxSonar-WRMLT [8]

The sonar sensor establishes a "ground truth" that allows the laser's distance measurements to be converted to account for the angle of refraction through the water column.

3.2.3 Inclinometer

When StreamScope is mounted by cable from nearby structures over streams, it allows for the possibility of the unit being tilted or rolled away from being perpendicular to the water's surface. Because of this, it becomes important to have a sensor that can accurately read the angles that the servo moves to if they do not match-up with pre-calibrated values. Ultimately, an accelerometer was decided as the sensor of choice, specifically the Adafruit ADXL343.

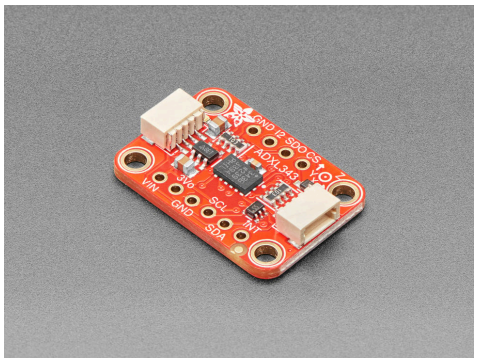

Figure 3.3: Adafruit ADXL343 - Triple-Axis Accelerometer [9]

The ADXL343 was chosen because of its low price and sufficiency for the application. While an IMU would also be sufficient, they also tend to be more expensive, and if the angle only has to be measured when the laser is at rest, then the accelerometer can calculate it accordingly using the following equation (when it is oriented vertically) [10]:

$$\theta = \tan^{-1}\left(\frac{a_y}{a_x}\right) \cdot \frac{180}{\pi}$$

Figure 3.4: Tilt Angle Calculation from Accelerometer Data

It has an Inter-Integrated Circuit (I^2C) interface for communication and offers many different resolutions for its output (+/- 2/4/8/12 g).

3.2.4 Servo Motor

The HiTec D646WP servo motor was chosen due to its waterproof design and its reputable manufacturer. It allows a wide range of operation voltages, allowing flexibility within the electrical design, and uses pulse width modulation (PWM) control to move to different positions.



Figure 3.5: HiTec D646WP Waterproof Servo [12]

3.2.5 Microcontroller

When choosing the microcontroller for StreamScope, it was important that it be easy to use, contained a wide variety of interfaces for communication between the sensors, and had extensive guidance online to allow those unfamiliar with embedded software to change parameters in StreamScope's code in the future.

The Teensy 4.1 was selected as the unit's microcontroller. The Teensy 4.1 contains an ARM Cortex-M7 clocked at 600 MHz, with the ability to under clock and sleep to save power [11]. It's onboard SD card reader allows for redundant datalogging functionality of both system information and sweeps. The built-in EEPROM allows for non-volatile storage of configuration values to influence StreamScope's behavior, such as site specific sweeps and information sent to the data logger. One of the most powerful hobbyist microcontrollers, the Teensy 4.1 provides plenty of memory and power to process large amounts of data.



Figure 3.6: Teensy 4.1 Microcontroller [11]

The Teensy 4.1 has support for the Arduino framework, which allows for accessible programming and extensive support compared to other microcontrollers that require more knowledge of embedded systems. Its design utilizes headers to connect to printed circuit boards, which allows it to be taken out and replaced in the event it becomes damaged.

3.3 Mechanical Design and Assembly

3.3.1 Scanning Module and Enclosure Design

Regarding the scanning mechanism, it was of the utmost importance that it be isolated from the outside environment. If this were not the case, debris could prevent the unit from scanning by blocking it from rotating.

To achieve environmental isolation for the scanning mechanism, the initial design of StreamScope employed a mirror-based system. A mirror was mounted at a 45-degree angle to the servo, with the laser aimed at its center, allowing the beam to scan downward through a cross-section of clear cylindrical acrylic tubing fixed to a junction box. While this configuration successfully protected the scanner from external elements, it introduced several significant challenges. The design required multiple precise cutouts with tight tolerances, making the system difficult to waterproof and replicate. More critically, the laser consistently reflected off the inner surface of the

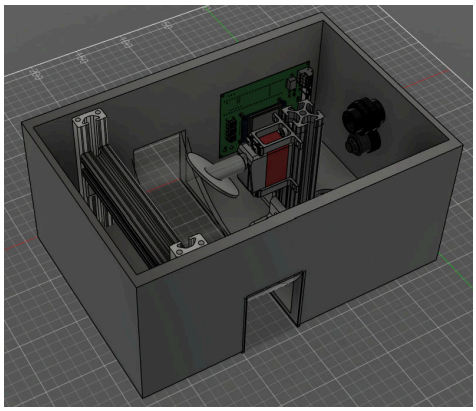

(a) Initial StreamScope CAD

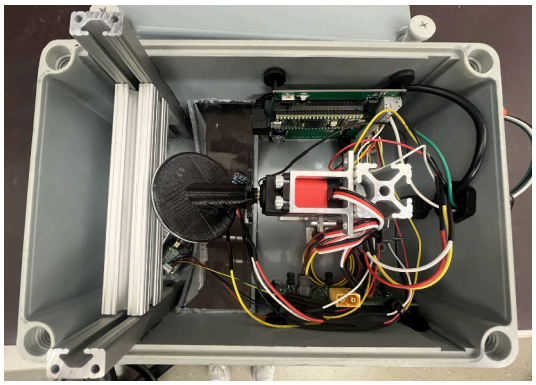

(b) Inside of Initial StreamScope Enclosure

Figure 3.7: Initial StreamScope Design

acrylic tubing rather than penetrating it, rendering the system ineffective for actual scanning.

As a result of this discovery, the following changes were required:

- Orient the laser as close to the acrylic as possible to prevent surface returns
- Make the scanning mechanism isolated from the electronics, more modular, and require less modifications to attach it to the enclosure to help with waterproofing and repeatability

To align with the project's goals of cost-effectiveness and simplicity, a 3D-printed scanning module was developed as the preferred solution. This design can be easily mounted to the side of any junction box with adequate surface area, allowing for flexible and repeatable installation.

The module designed houses a 3.5-inch acrylic cylinder that fits into the main housing's inserts. An o-ring is pre-installed in these inserts to ensure waterproofing. The lid, featuring its own set of inserts, attaches securely on the opposite side using four screws. Installation onto the enclosure only requires four screws and a cutout for the servo, significantly reducing the modifications needed for the junction box. A

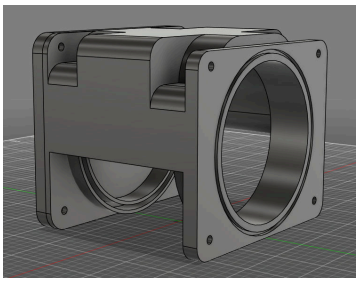

(a) Scanning Module CAD Assembled

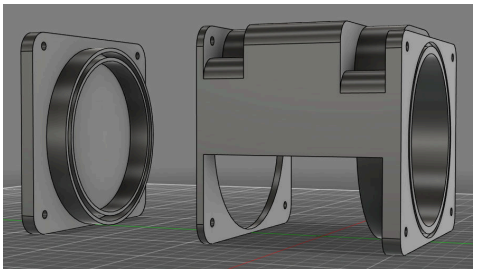

(b) Scanning Module CAD Side View

Figure 3.8: Scanning Module CAD

small recess on the back of the module accommodates an o-ring or rubber gasket for additional sealing. The servo is fastened in place with sealant applied around its edges. To route wires for the laser and accelerometer, a compact cable gland is positioned above the servo.

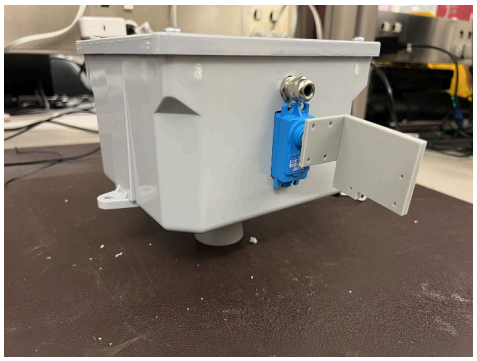

(a) Servo and Cable Gland Installation

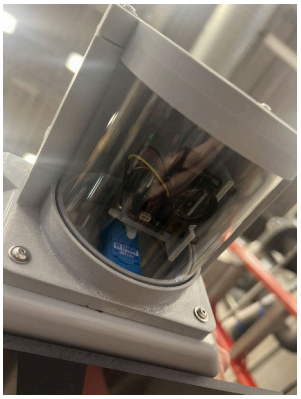

(b) Scanning Module Underside View

Figure 3.9: Scanning Module

The module was printed with polyethylene terephthalate glycol (PETG) filament, as it is easily printed on low-cost 3D printers and has a higher heat deflection temperature than the more common polylactic acid (PLA) filament, making it less prone to sagging under warmer conditions [6]. One of the issues with 3D printing parts for outdoor use is that they are printed in layers, which causes gaps that can allow water to either

build inside the hollow walls of the print and swell, or even lead to leaks. To combat this, the following steps were taken:

- Printed slower and at a higher temperature than suggested to ensure layer adhesion and to keep layer gaps as small as possible.
- Increased the number of walls and percentage infill to provide a strong barrier from outside elements and to improve long term durability.
- Coated the outside in FlexSeal Clear™ to seal any remaining gaps as an extra precaution.

The module was mounted onto a 6x6x4 inch Cantex™ junction box. To confirm its waterproof effectiveness, an outdoor experiment was conducted. After several days of exposure to rain, the unit continued to operate as intended, with no evidence of moisture accumulation inside the tubing and the main compartment.



Figure 3.10: Scanning Module After A Rainstorm

The servo mount, designed to hold both the laser distance module and accelerometer, was also 3D printed using PETG. The accelerometer is precisely centered on the servo's output shaft to ensure accurate angle measurements. The laser distance module is mounted facing downward on standoffs, carefully aligned with the accelerometer.

Since most 3D printers cannot reliably produce the fine details required for 25-tooth (25T) servo attachments, a pre-made 25T servo gear was superglued to the back of the mount to enable proper connection to the servo.

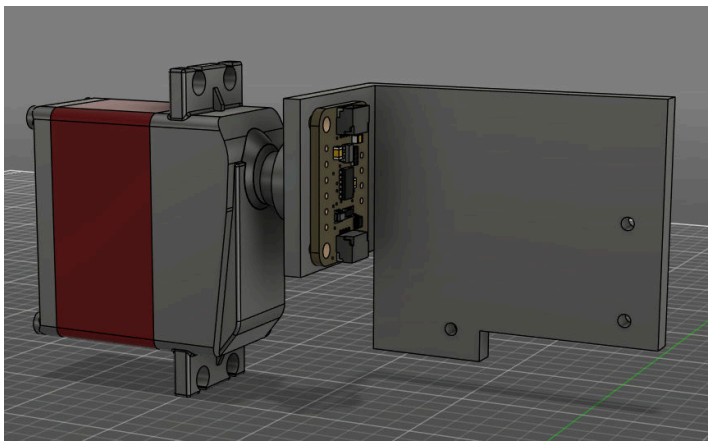

Figure 3.11: Servo Attachment

Outside of the scanning mechanism, a hole was drilled in the bottom center of the unit to accommodate the sonar, which was secured from the inside using an o-ring and a 3/4-inch steel lock nut. To eliminate the need for multiple small holes for the PCB stand-offs, 3D printed plates with M2 inserts were fabricated and mounted to the sides of the enclosure to hold the stand-offs. At the back of the enclosure, a final hole was drilled for a cable gland. Additionally, a counterweight was added around this hole to help the unit maintain its balance independently.

Separating the scanning mechanism from the main enclosure, which houses most of the electronics, enhances the overall waterproofing. This design keeps modifications to the main enclosure minimal and easy to seal. In the event of a leak within the scanning module, the electronics in the main enclosure remain protected, allowing them to continue operating and alert the datalogger of the malfunction.

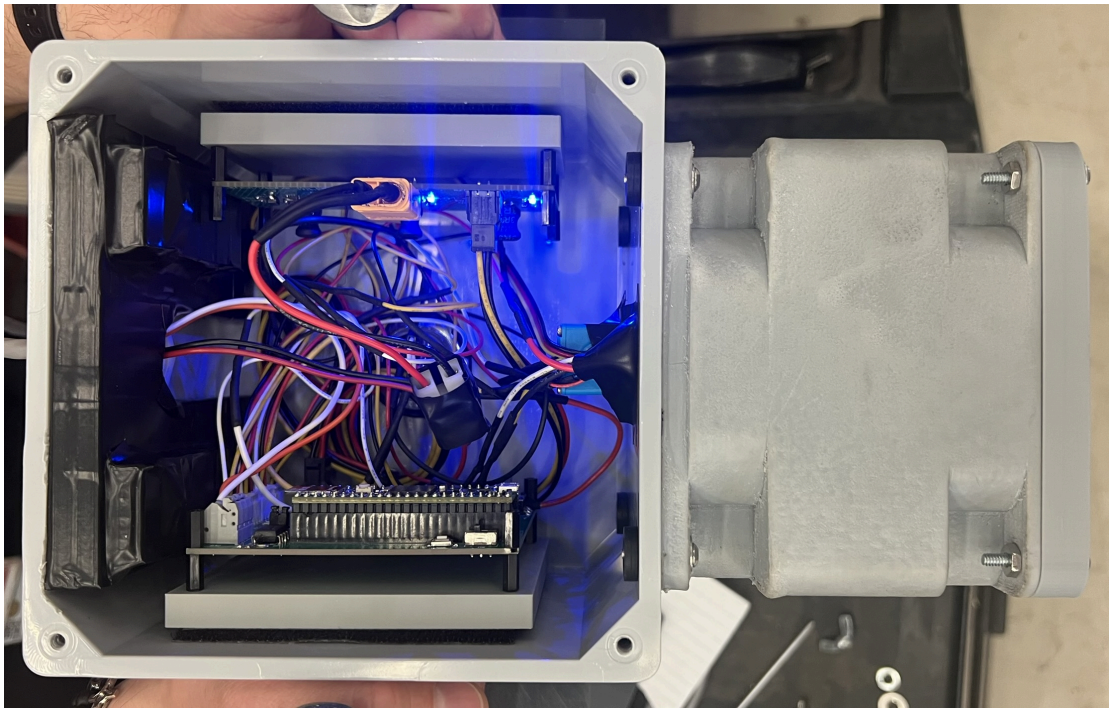

Figure 3.12: Top-Down View of StreamScope

3.3.2 Mounting Configuration

The Cantex™ junction box features screw holes on the bottom edges of each side, which were used to design a non-invasive mounting harness for the unit, avoiding the need to drill holes in the lid.

Two plates were fabricated—one for the top and one for the bottom. Two metal pipes were cut, bent, flattened, and drilled to connect the plates. The screws are fastened using lock nuts. The top plate can be customized by drilling mounting holes as needed, eliminating the need to drill directly into the enclosure's lid.



Figure 3.13: StreamScope Mounting Configuration

3.4 Printed Circuit Board Design

The printed circuit boards designed for StreamScope emphasize ease of assembly and reliability. To simplify soldering, only components with readily accessible package sizes were chosen, avoiding integrated circuits with small or hard-to-solder formats. Locking connectors were used for all interfaces to prevent cables from loosening due to movement, ensuring stable connections during operation. This connector-based design also streamlines assembly, making it easy to connect and disconnect each interface.

The electrical system is divided into two boards: one dedicated to controlling all peripherals and communicating with the datalogger, and the other focused on efficiently stepping down the supplied 12-volt power to the 7V, 5V, and 3.3V levels required by the peripherals.

Separating the system into two boards provides modularity and enhances overall reliability. Isolating power regulation on a dedicated board allows for better thermal management and electromagnetic interference (EMI) control without impacting the more sensitive signal and control components. This division also simplifies troubleshooting and future upgrades, as power-related issues can be addressed independently from the control logic. Moreover, it enables optimized layout and component placement tailored to each function—power converters can be designed with appropriate clearances and heat dissipation, while the control board can focus on maintaining signal integrity and communication performance.

3.4.1 Power Distribution Board

The power distribution board is responsible for stepping down a 12V input to 7V, 5V, and 3.3V using three dedicated buck converters.

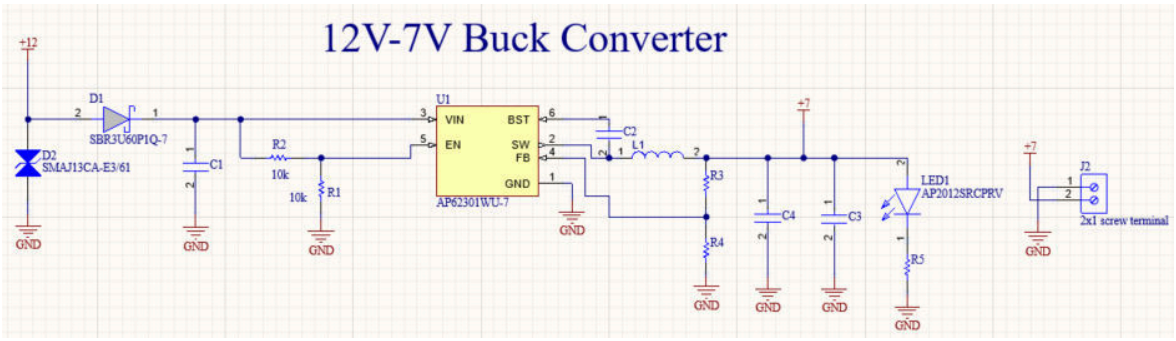

Figure 3.14: Power Distribution Schematic (7V Buck Converter)

An XT60 connector provides a secure and high-current connection for the 12V input. To protect each converter from electrical transients and reverse polarity, a Schottky diode and a transient voltage suppression (TVS) diode are placed on the input of each buck regulator. The regulated outputs are delivered to the main control

board via a four-pin Molex™ connector carrying 7V, 5V, 3.3V, and GND. Three optional screw terminals were included onboard for each output for redundancy purposes. Buck converters were chosen over linear regulators due to their significantly higher efficiency, which is especially critical in a solar-powered, remotely deployed system where minimizing energy loss is essential for maximizing uptime and reliability.

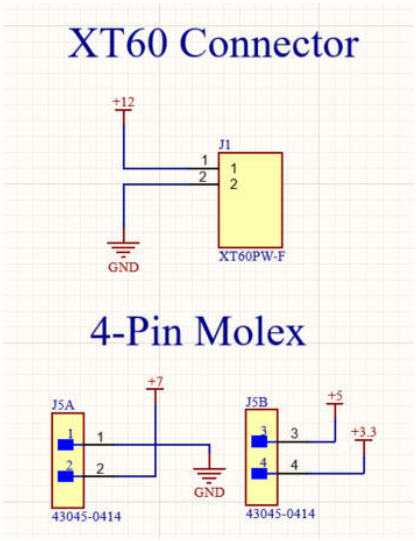

Figure 3.15: Power Distribution Schematic (Outputs)

The PCB is a two-layer design using 2 oz copper, chosen based on the buck converters' datasheet recommendations to ensure proper heat dissipation and support the required current load. Both layers feature a stitched ground pour, creating a low-impedance ground path to reduce electrical noise and enhance signal integrity. Polygon pours are used to connect the input and output pins of each buck converter, minimizing trace resistance and improving power delivery efficiency. Although a four-layer board was considered, the two-layer design met all electrical and thermal requirements while keeping costs lower.

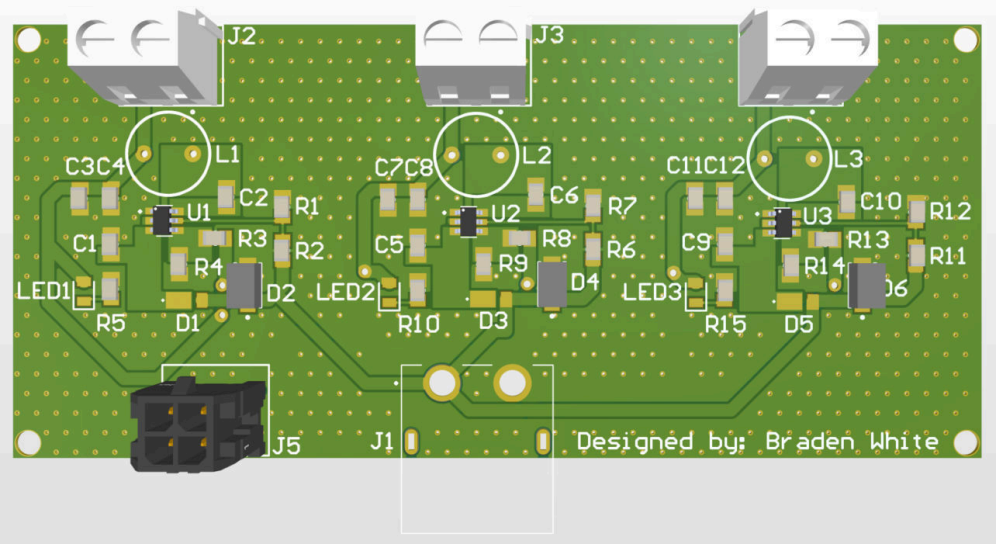

Figure 3.16: Power Distribution 3D Model

3.4.2 Control Board

The control board is built around a Teensy 4.1 microcontroller, which manages all connected peripherals. It receives 7 V, 5 V, and 3.3 V power from the distribution board through a four-pin Molex connector. The accelerometer communicates via I^2C, while the laser and sonar modules have UART interfaces. The servo is controlled with a PWM signal. All peripherals are connected using JST™ locking connectors instead of screw terminals, providing secure and reliable connections suitable for rugged environments. For communication with the datalogger or a Raspberry Pi, the board includes an onboard RS-485 transceiver and uses a latching connector to support the Modbus protocol.

Decoupling capacitors are placed at each integrated circuit to stabilize voltage levels and suppress electrical noise, while bulk capacitors are positioned near the servo to manage its high transient current demands. To optimize power usage, each peripheral is individually powered by switching its ground connection using metal oxide semiconductor field-effect transistors (MOSFETs). Since the sonar module operates

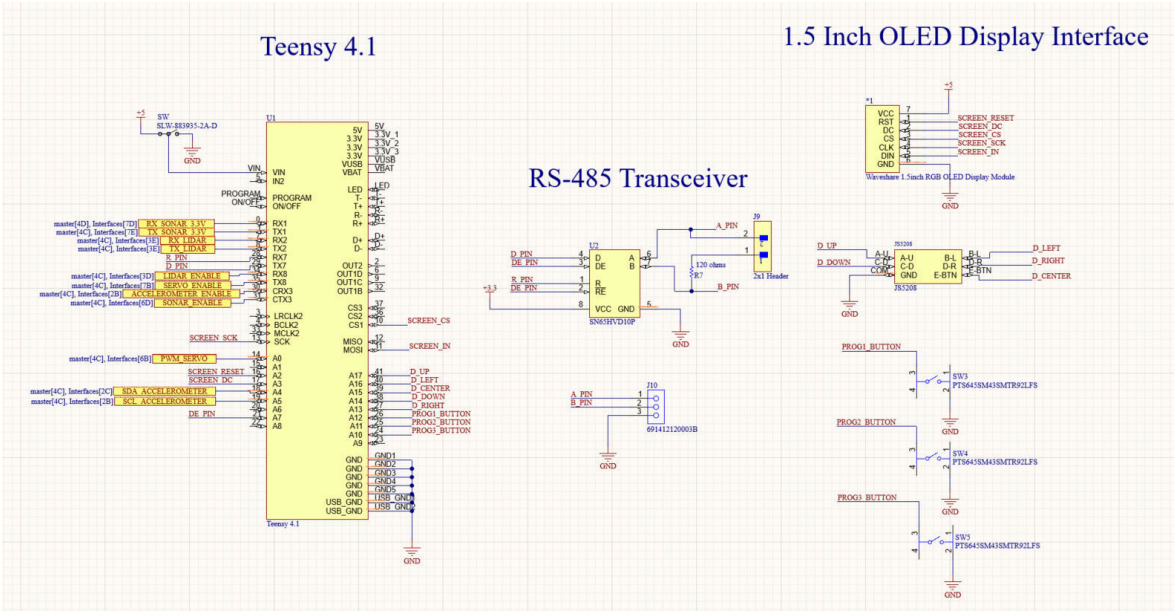

Figure 3.17: Control Board Schematic (Page 1)

at 5V logic, a level-shifting MOSFET circuit is used to convert signals between the Teensy's 3.3V logic and the sonar's 5V logic. Additionally, a dedicated power switch is included to control power to the Teensy, protecting it from potential damage caused by simultaneous USB and external power source usage.

Regarding the board layout, all interfaces were placed on one side to organize wiring neatly in a single row rather than scattered across the board. The board is a two-layer design chosen to reduce cost, using 1 oz copper on both layers. The bottom layer is dedicated to a ground pour to provide a stable reference and minimize noise, while the top layer includes power pours for each voltage supply to efficiently distribute power to components.

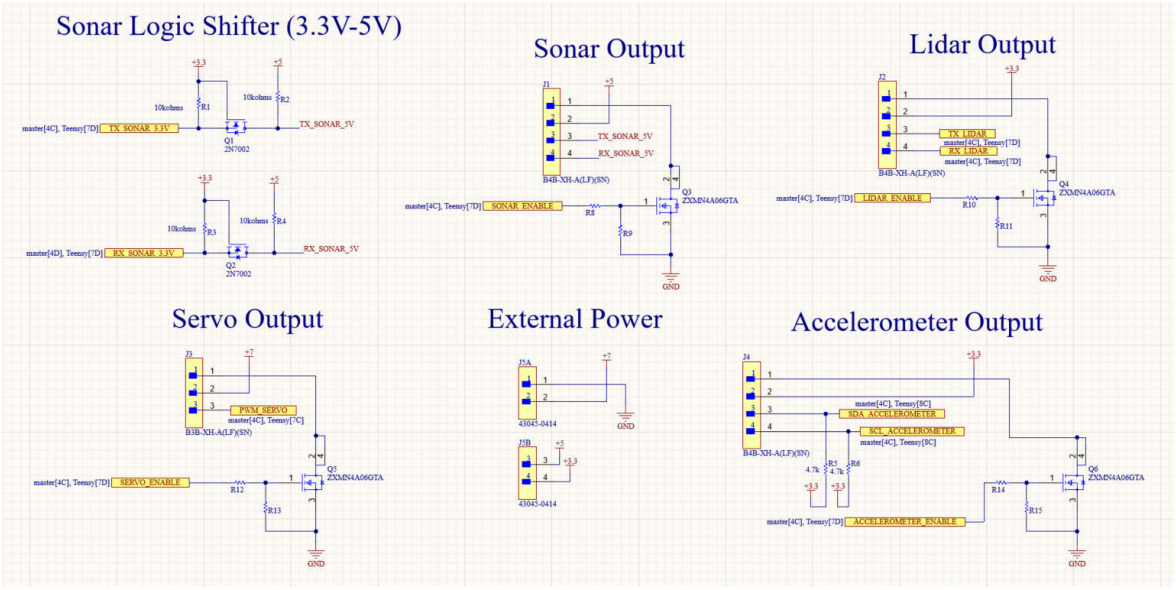

Figure 3.18: Control Board Schematic (Page 2)

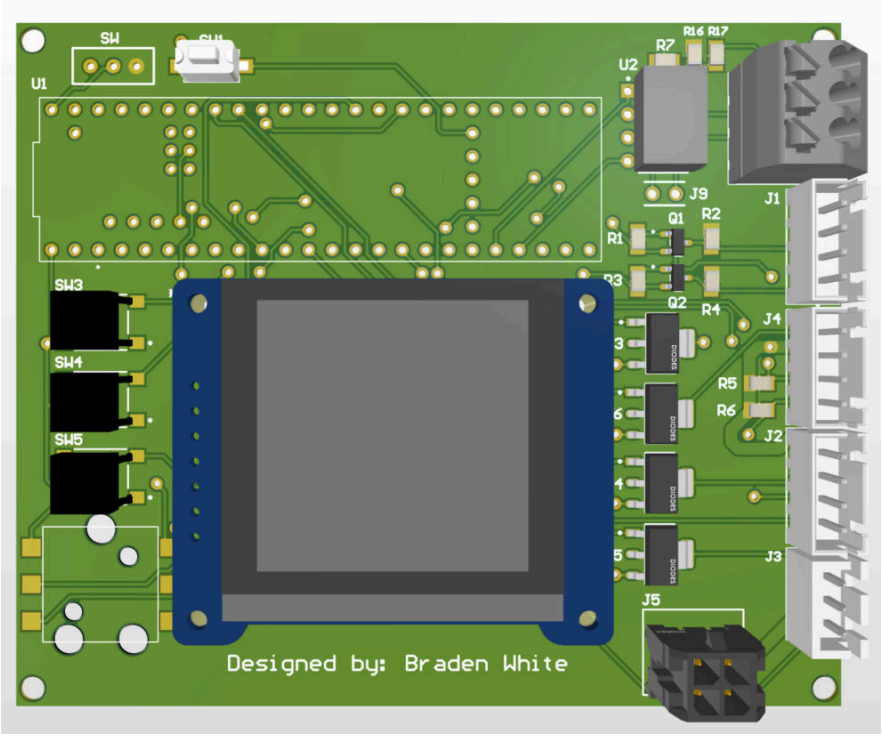

Figure 3.19: Control Board 3D Model

3.5 Firmware

The firmware for StreamScope is built using the Arduino framework, chosen not only for its flexibility but also to facilitate future maintenance and development by the USGS. This widely adopted framework simplifies hardware abstraction and integration with sensors and communication interfaces, making the codebase more accessible to engineers and technicians who may work with the system later. The firmware orchestrates sensor triggering, data acquisition, peripheral control, and communication with the datalogger, ensuring reliable and synchronized operation throughout the scanning process.

3.5.1 Modbus RS-485 Communication

For communication between StreamScope and external devices, two protocols were considered: Modbus over RS-485 and SDI-12. Modbus RS-485 was chosen due to its higher data throughput, greater configurability, and more versatile options for data exchange. Unlike SDI-12, which is primarily designed for simple sensor networks with limited data rates and command sets, Modbus offers a robust and widely adopted industrial standard that supports complex queries. The use of RS-485 as the physical layer ensures noise-resistant communication over longer distances, making this combination well-suited for the conditions of remote environmental monitoring.

In this system, registers are carefully allocated to represent key measurement data, status indicators, and control inputs. For example, registers may include current scan parameters, distance measurements, system status flags, and configuration options such as sweep type or measurement intervals. This structured mapping ensures efficient data retrieval and simplifies integration with external software by providing a clear interface to the instrument's operational data.

```
const uint16_t UPDATE_TIME_REG = 0;
const uint16_t CURR_HOUR_REG = 1;
const uint16_t CURR_MIN_REG = 2;
const uint16_t CURR_DAY_REG = 3;
const uint16_t CURR_MONTH_REG = 4;
const uint16_t CURR_YEAR_REG = 5;
const uint16_t SWEEP_TYPE_REG = 6;
const uint16_t NUM_MEASUREMENTS_REG = 7;
const uint16_t NUM_ANGLES_REG = 8;
const uint16_t NUM_SWEEPS_REG = 9;
const uint16_t MEASUREMENTS_READY = 10;
```

Figure 3.20: Sample of Modbus Registers Used for StreamScope

This register-based architecture provides fully configurable control over the system's behavior without the need to reprogram the firmware. Users can remotely adjust operational parameters, trigger specific functions, or access real-time data simply by modifying register values. This approach offers a high degree of flexibility and adaptability, allowing the system to be easily tailored to different deployment scenarios.

3.5.2 Scanning Pipeline

The scanning pipeline governs the core operation of the StreamScope system, coordinating the interactions between hardware peripherals and software routines to execute accurate, efficient, and reliable measurements. This process encompasses initializing key devices, managing communication protocols, conducting measurement sweeps, processing collected data, and logging results—all while maintaining system stability and safeguarding against errors in challenging field conditions.

3.5.2.1 Initialization

The firmware begins by configuring the hardware pins responsible for enabling each peripheral device, including the laser, sonar, accelerometer, and servo. An optional debug LED pin is also configured if debug mode is enabled.

Next, the Modbus RTU server is initialized with a device ID of 1 and a baud rate of 19200, the standard speed commonly used for Modbus over RS-485. The holding registers are then allocated to store both configuration settings and real-time operational data.

Pre-configured sweep information is then loaded from EEPROM memory with its parameters such as the number of measurement angles and total measurements per sweep. These parameters are written back into the Modbus holding registers so that the datalogger can access the currently configured values.

The internal temperature sensor is initialized to continuously monitor the system's thermal conditions, ensuring reliable operation and providing critical status updates to the datalogger via Modbus registers. A hardware timer periodically triggers a routine that reads the temperature and adjusts the processor's clock speed accordingly. When the system is idle, the processor is underclocked to 24 MHz to conserve power. If the temperature rises above predefined thresholds, the clock speed is further reduced to prevent overheating. During active operation, the processor runs at its full 600 MHz but will automatically scale down if temperatures exceed safe limits. This adaptive clock management strategy ensures a balanced trade-off between performance, energy efficiency, and thermal protection.

```
void variableClock() {
    temperature = InternalTemperature.readTemperatureC();
    uint16_t modTemp = static_cast<uint16_t>(temperature + 32768);
    ModbusRTUServer.holdingRegisterWrite(TEMPERATURE_REG, modTemp);
    if (idle) {
        if (temperature > 20) {
            set_arm_clock(_24MHZ);
        } else if (temperature > 10) {
            set_arm_clock(_150MHZ);
        } else if (temperature > 0) {
            set_arm_clock(_450MHZ);
        } else {
            set_arm_clock(_600MHZ);
        }
    } else {
        if (temperature < 50) {
            set_arm_clock(_600MHZ);
        } else if (temperature < 60) {
            set_arm_clock(_450MHZ);
        } else if (temperature < 70) {
            set_arm_clock(_150MHZ);
        } else {
            set_arm_clock(_24MHZ);
        }
    }
}
```

Figure 3.21: Variable Clock Speed Routine for the Teensy 4.1

If debug mode is enabled, the firmware sets a debug flag in the Modbus registers to notify the datalogger and initializes the serial interface, outputting key system information such as the CPU frequency and initial temperature reading.

Finally, the SD card interface attempts to initialize. Once the setup tasks are completed, the firmware enters its main loop to manage Modbus communication, measurement acquisition, data processing, and logging operations. The conditions in which each function in the main loop are called are:

- `modbus()`
  - The Modbus RTU server has incoming data to poll (`ModbusRTUServer.poll()` returns true), **or**
  - New Modbus measurements are ready to be processed (`modbusMeasurementsReady` is true).
- `measure()`
  - The measurement queue is not empty (`!measurementQueue.isEmpty()`), **and**
  - A sweep is not currently in progress (`!sweepInProgress`).
- `process()`
  - A sweep has finished (`sweepFinished` is true).
- `sdCard()`
  - The SD card has been successfully initialized (`sdCardInitialized` is true), **and**
  - The measurements are ready to be logged (`measurementsReady` is true).

3.5.2.2 Polling Modbus

When the firmware enters the `modbus()` function, it checks certain registers that are used to initiate tasks, such as:

- `UPDATE_TIME_REG`: Update the internal stored time for onboard logging.
- `SWEEP_TYPE_REG`: Initialize a new measurement sweep. The type depends on the register's value.

- `EEPROM_INITIALIZE_REG`: Initialize new EEPROM-configured measurement sweep.

When these flags change from their default value of zero, this signals to StreamScope that the particular operation has been requested. The flag is only changed by the datalogger after the holding registers are filled with the parameters required to carry out the command.

```
if (ModbusRTUServer.holdingRegisterRead(SWEEP_TYPE_REG) == 1) {
      if (debug) Serial.println("Message-General_Sweep");
      modbusMessage.sweepType =
          ModbusRTUServer.holdingRegisterRead(SWEEP_TYPE_REG);
      modbusMessage.numAngles =
          ModbusRTUServer.holdingRegisterRead(NUM_ANGLES_REG);
      modbusMessage.numMeasurements =
          ModbusRTUServer.holdingRegisterRead(NUM_MEASUREMENTS_REG);
      modbusMessage.numSweeps =
          ModbusRTUServer.holdingRegisterRead(NUM_SWEEPS_REG);
      ModbusRTUServer.holdingRegisterWrite(SWEEP_TYPE_REG, 0);
      measurementQueue.enqueue(modbusMessage);
      if (debug) Serial.println("Enqueued-General_Sweep");
}
```

Figure 3.22: Conditional Statement for a General Sweep

Whenever a sweep is requested, the sweep is placed in a queue where it will be popped in the `measure()` function and carried out accordingly.

In addition to this, the `modbus()` function also carries out the process for sending back sweep information if the last sweep's data is ready for transmission.

3.5.2.3 Conducting a Sweep

Whenever a sweep is detected in the the `measurementQueue`, the `measure()` function is called. This function is responsible for managing the scanning process, including powering on the necessary peripherals, moving the servo to the correct angles, and collecting measurements from the laser range finder. For each sweep, a `LidarSweep` structure that contains `LidarMeasurement` structures is created. The `LidarMeasurement` structure contains all of the information collected at a single angle, including the distance

reading, the servo angle it was taken at, the accelerometer angle, and the coordinate point adjusted for the Snell's Law if applicable. Besides containing a vector of the measurement objects, the `LidarSweep` structure contains the sonar distance reading, time the sweep was conducted, and the status of the sensors during the sweep.

StreamScope contains four different modes of conducting a sweep:

- **General Sweep:** User inputs the number of angles and the number of measurements at each angle. The angles at which measurements are taken are evenly spaced and distributed across the full width of the scanning mechanism's allowed range. This mode is intended to be used in situations where data transmission is constrained or if battery power is a commodity, but the majority of the stream is within StreamScope's field of view.

- **Specific Sweep:** User inputs the number of angles, measurements, and also the specific angle values. This mode is intended to be used in the event data transmission is constrained or if battery power is a commodity, but the stream is not centered to StreamScope's field of view.

- **Configured Sweep:** User prompts StreamScope to scan according to its stored values in EEPROM. This can be used to simplify the datalogger's requests for a measurement by storing the parameters ahead of time.

- **Full Sweep:** User prompts StreamScope to scan at every possible angle, which is typically $\pm$ 50° from nadir, the center of the stream. At an ideal site where battery power is plentiful, this mode offers the best resolution and bathymetric fidelity.

After the sweep is popped from the queue, the associated digital output pins that actuate the MOSFETs are driven high to turn the peripherals on and their respective

communication protocols are initialized. Once this is finished, the `measurementSweep()` function is called, which handles carrying out the sweep.

After collecting the sonar reading to establish the distance to the surface of the water, the sweep can then be conducted. The servo moves the laser according to the requested sweep and is constrained by a lower angle constraint and an upper angle constraint to prevent from scanning upward or inside the unit in the event of an erroneous value sent.

After the servo moves to a new angle in the sweep, the angle is determined using the accelerometer. Because accelerometer readings can be noisy, multiple samples are taken and processed through a low-pass filter to remove high-frequency noise. This filtering ensures that the angle feedback is accurate and reliable.

```
accelerometer.getEvent(&event);
float accel_x = event.acceleration.x;
float accel_y = event.acceleration.y;
float angle = atan2(accel_y, accel_x) * 180 / PI;
filteredAngle = alpha * angle + (1 - alpha) * filteredAngle;
```

Figure 3.23: Low Pass Filter for Angular Feedback

The Egismos laser range finder supports two primary operating modes: continuous measurement and single measurement. In continuous mode, the laser continuously outputs distance readings as long as it remains powered, enabling rapid data collection. In single measurement mode, the laser returns a distance reading only when explicitly triggered. By default, StreamScope operates in continuous mode. However, if single measurement mode is preferred, the datalogger can specify this by setting the appropriate holding register when initiating a sweep, allowing StreamScope to switch modes accordingly.

Once the sweep is complete, the servo is moved back to its resting position, the peripherals are turned off, and the sweep's `sweepFinished` flag is changed to true. The measurements are then placed in a queue to be processed in the `process()` function.

3.5.2.4 Processing Measurements

The `process()` function is called when a sweep is finished. It is responsible for processing the measurements collected during the sweep, including applying coordinate transformations and converting measurements into a format compatible with Modbus communication.

For each angle and distance pair, the function computes the corresponding coordinate point. The x-coordinate is derived from the distance reading and the angle, while the y-coordinate is based on the sonar reading and the angle. When the y-coordinate is less than the sonar reading, Snell's Law is applied to adjust the y-coordinate, accounting for the water's refractive index (1.33) and the angle of incidence. If the point is determined to be located outside of the water, it's polar coordinates are converted to Cartesian coordinates without further calculations. Both coordinates are then multiplied by -1 to invert the coordinate system, aligning the points with the reference frame where the laser is positioned above the water and scanning downward.

These calculated coordinates are then stored in the `rawPoints` vector for later use.

Modbus holding registers require unsigned 16-bit integers. This means that the values that its registers can hold range from 0 to 65535. To accommodate the negative values that can occur in the coordinates and angle values, these values are offset by 32768, allowing them to be stored as unsigned integers. The resulting values are stored in similarly named data structures with the suffix "UINT16" appended to their names.

```
double n1 = 1.00;
double n2 = 1.33;
double waterLevel = meas.sonarDistance;
double radAngle = std::radians(meas.angle);

for (size_t i = 0; i < meas.distances.size(); ++i) {
    double dist = meas.distances[i];
    if (dist > 500 && dist < SITE_LIMIT) {

        double dA = waterLevel / std::cos(radAngle);
        double dB = dist - dA;

        if (dB <= 0) {
            double xA = std::sin(radAngle) * dist;
            double yA = std::cos(radAngle) * dist;
            meas.rawPoints.emplace_back(-xA, -yA);
        } else {
            double beta = std::asin(n1 * std::sin(radAngle) / n2);
            double xA = std::sin(radAngle) * dA;
            double xB = std::sin(beta) * dB / n2;
            double yB = std::cos(beta) * dB / n2;
            meas.raw_points.emplace_back(-(xA + xB), -(waterLevel + yB));
            meas.inWater = true;
        }
    }
```

Figure 3.24: Calculating Coordinate Points Using Snell's Law

3.5.2.5 SD Card Logging

The `sdCard()` function is responsible for logging the measurements to the SD card. It is called when the SD card has been initialized and the measurements are ready to be logged. The function logs the measurements to a text file in a comma-separated format, including the date, time, and all the measurements collected during the sweep. The file is named using the current date and time to ensure uniqueness and easy identification.

```
----------------------------------------
      StreamScope Sweep Log File
----------------------------------------

Date: 08/06/2025
Time: 11:17 UTC

----------------------------------------
          Sweep Details
----------------------------------------

Number of Angles: 101
Number of Measurements at Each Angle: 30
Requested Angles (degrees): Full Sweep
```

Figure 3.25: StreamScope Log File

3.5.3 Safeguards and Fail-Safes

Developing a system that is intended to be deployed in the field for long periods of time requires careful consideration of potential failure modes and safeguards to ensure reliability. StreamScope implements several fail-safes in its firmware to mitigate risks associated with hardware and software failures:

- **Laser Module Stall Detection:** When the laser module is in continuous measurement mode, it is possible for the laser to become stalled if it is unable to receive a strong return signal. The laser itself will retry until it is able to return a valid measurement. To avoid long delays in the event of a stall, the firmware implements a timeout mechanism that will effectively skip the measurement by recording a distance of 9999. This not only ensures that the scanning process can continue without being indefinitely delayed, but it also helps save power by not keeping StreamScope on for longer than necessary.

- **SD Card Initialization Retry:** An issue arose during testing where the SD card initialization would occasionally fail, despite there being nothing wrong with the interface. The SD card is initialized at startup, and if initialization fails, the firmware will retry three times before giving up and logging an error message to a Modbus register. By retrying the initialization, the system can recover from transient errors that may occur during startup.

- **Soft Reset:** If StreamScope either stalls or given large measurement values on accident, the firmware allows the user to perform a soft reset by writing to a specific Modbus register. This will reset the Teensy microcontroller and reinitialize the system, allowing it to recover from any unexpected states without requiring physical intervention. This is accomplished by the firmware including consistent calls to the `modbus()` function in any loop that has the capacity to stall

to see if any Modbus registers have been modified, including the reset register. If the reset register has been modified, the firmware will reset the Teensy and reinitialize the system.

- **Redundant Sonar Readings:** The sonar module is polled multiple times during a sweep to ensure that the reading is accurate. That way if the first reading is erroneous, the system can still use a valid reading to calculate the coordinate points. The sonar module is polled at least three times, and if all three readings are invalid, the system will log an error message to a Modbus register to inform the datalogger and continue with the sweep.

- **Modbus Configuration Registers:** To prevent the firmware from having to be reprogrammed, the vast majority of values or parameters can be modified through Modbus registers.

- **EEPROM Configuration:** The EEPROM is used to store configuration values that are not intended to change frequently, such as the number of angles and measurements per sweep. This allows the system to retain its configuration even after a power cycle, ensuring that it can resume operation without requiring reconfiguration.

3.6 Data Post-Processing

After the data from a sweep is sent to a nearby datalogger or Raspberry Pi, it is then processed to calculate the cross-sectional area of the stream and to create a bathymetric map. The post-processing includes several main steps: cleaning up noisy data, finding key points (centroids) that represent important features, identifying the left and right banks of the stream, and calculating the cross-sectional shape and area of the riverbed.

These steps turn the raw measurements into useful information about the flow and shape of the stream.

3.6.1 Centroid Estimation Using 2D Kernel Density Estimation

In order to accurately extract meaningful features from sometimes noisy laser returns, a centroid estimation technique based on two-dimensional Kernel Density Estimation (KDE) was implemented. This approach allows for a probabilistic interpretation of point concentration by estimating the probability density function (PDF) over the spatial distribution of raw laser distance returns for each angle of a given sweep.

This process requires a two-dimensional KDE because of the effects of Snell's Law, which causes measurements taken through the water column to be refracted and change trajectory. As a result, the spatial distribution of the returns is no longer constrained to a perfect radial line. Instead, points may exhibit spread in both the horizontal and vertical directions because of the change in refractive index. Furthermore, in the event that multiple measurement sweeps are utilized during post-processing, the sonar-measured depth can change between sweeps, altering the path length through water and thus affecting the effective index of refraction experienced by the laser's beam.

Using Scikit-learn's KernelDensity module with a Gaussian kernel, the PDF was estimated over the spatial coordinates. A bandwidth parameter controls the smoothness of the kernel and can be adjusted according to the characteristics of the sweep.

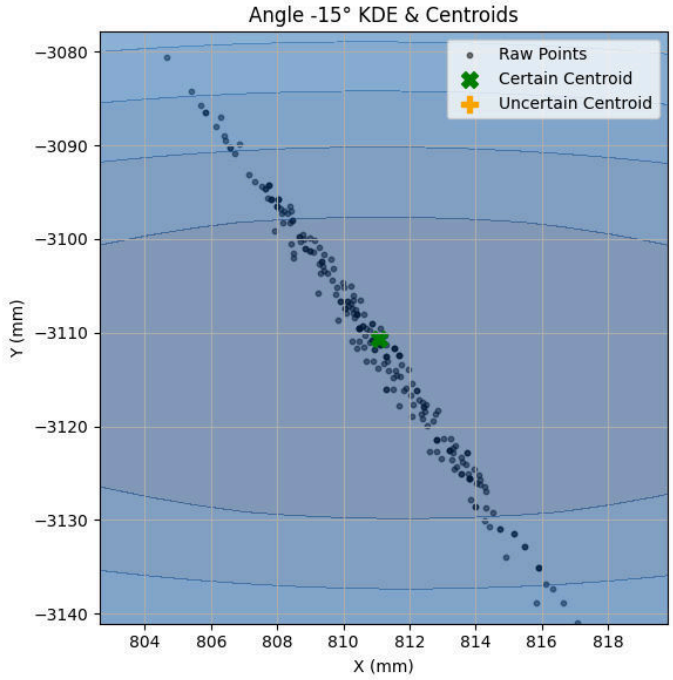

Figure 3.26: Return Differences at the Same Angle Over Multiple Consecutive Sweeps

To evaluate the density function, a uniform grid was generated across the bounding box defined by the minimum and maximum x and y coordinates of the point cloud. The KDE model was then used to score each point in this grid, producing a log-density map representing the likelihood of point concentration across space.

```
from sklearn.neighbors import KernelDensity
kde = KernelDensity(kernel='gaussian', bandwidth=bandwidth).fit(coords)

x_min, y_min = coords.min(axis=0)
x_max, y_max = coords.max(axis=0)
x_grid = np.linspace(x_min, x_max, 100)
y_grid = np.linspace(y_min, y_max, 100)
xx, yy = np.meshgrid(x_grid, y_grid)
grid_points = np.vstack([xx.ravel(), yy.ravel()]).T
log_density = kde.score_samples(grid_points)
log_density_2d = log_density.reshape(xx.shape)
```

Figure 3.27: 2D Kernel Density Estimation With a Gaussian Kernel

To detect significant features in the density map, a peak detection mechanism was employed. A maximum filter with a configurable neighborhood size was applied

to identify local maxima in the density field. These peaks correspond to the densest regions of the respective angle's point cloud and serve as candidate centroids. The peaks were labeled and the most prominent peak—i.e., the global maximum—was selected as the certain centroid. This point is presumed to be the most reliable estimate of a central object or surface detected by StreamScope.

In addition to the primary peak, a secondary analysis was performed to extract what is called an uncertain centroid. In environments affected by excessive water surface reflection or high turbidity, a possibility that may occur is receiving fewer valid distance measurements that originate from below the water's surface than at the water's surface. Because of this, the uncertain centroid serves as a secondary hypothesis for submerged object detection when the certain centroid may be biased by environmental interference. In Fig. 3.28, the certain centroids (green) near 0° were located at the surface. After those measurements were removed through a pruning process discussed in Section 3.6.2, the uncertain centroids (yellow) fill the gap and provide a physically plausible estimate of submerged target locations.

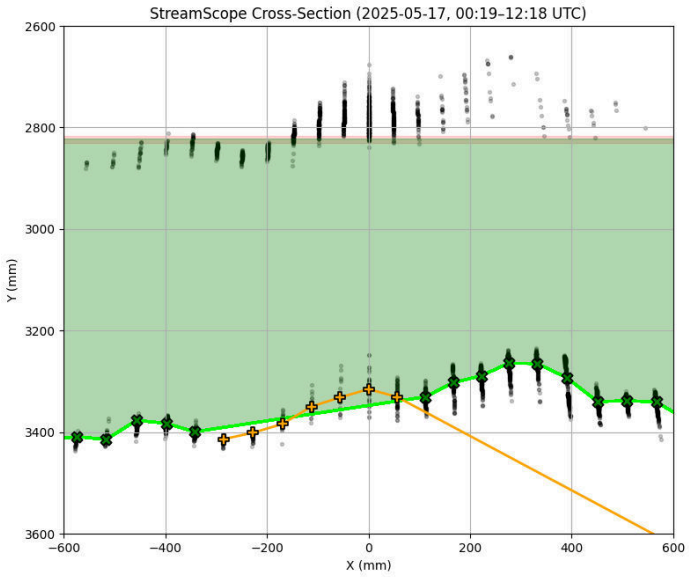

Figure 3.28: Uncertain Centroids Filling the Gap Around 0° for a Cross-Section

A heuristic filter was applied to secondary peaks to improve accuracy: any peak with a vertical distance closely matching the sonar measurement was de-prioritized. Only peaks exhibiting a vertical deviation greater than a specified threshold below the sonar reading were considered as viable uncertain centroids. This threshold is adaptable and typically increases with the depth of the stream, varying according to site-specific conditions.

By estimating where points are most concentrated, utilizing a 2D Kernel Density Esimate with a Gaussian kernel can better handle multiple objects and noisy data. It helps identify the main surfaces more clearly, even when some points are scattered or partially hidden.

3.6.2 Locating the Left and Right Bank Coordinates

In order to accurately segment and interpret features within a stream's cross section, it is essential to determine the spatial extent of the water body. This process begins with the identification of the left and right bank coordinates, which serve as spatial anchors for bounding the in-water region and constraining further analysis to relevant areas.

The left and right banks are typically identified as the outermost lateral extents of the certain centroids that satisfy specific criteria, such as having a vertical position (y-coordinate) that is shorter than the sonar distance retrievals. These coordinates represent the transition points from water to land and are crucial for defining the effective horizontal limits within which submerged targets or bathymetric features are expected to occur.

In implementation, the banks are located by scanning the point cloud from either end of the angular sweep and stopping at the first certain centroid that occurs at a distance longer than the sonar returns, signifying it is most likely located in the water column. The certain centroid immediately before the first in-water detection is most likely to represent one of the stream banks. In environments with well-defined shorelines, this method is generally robust; however, in dynamic or low-return environments, heuristic or manual strategies may be required.

3.6.3 Pruning Consistent, Erroneous Measurements

Following the initial centroid estimation process, a secondary filtering step is employed to prune centroid detections that are likely to be erroneous or physically implausible. These systematic artifacts—often appearing consistently across sweeps—can arise from misclassified water surface returns or noisy measurements in shallow, cluttered, or

highly reflective environments. These kinds of environments will be observed in more detail throughout Chapter 4 and Chapter 5. This pruning process incorporates both the sonar distance measurements and river bank estimations to constrain centroid detections to physically plausible regions within the channel.

Certain centroids are first removed if they fall spatially between the left and right bank boundaries and exhibit a vertical distance (in the y-direction) shorter than the reference sonar depth, suggesting that they may be surface reflections or intermediary structures rather than submerged objects. Additionally, centroids located within a small range of the sonar-determined water surface level that occur within $\pm 15^{\circ}$ of nadir are flagged and discarded, due to the high rate of erroneous surface reflections observed in experiments described in Chapter 4.

By enforcing the criteria for removal, if returns are somehow consistently at the water's surface or above it, they are removed to ensure that the cross-sectional area calculation only accounts for points retrieved from the bottom of the stream.

3.6.4 Cross-Sectional Area Calculation

To quantify the volume of flow and analyze channel morphology, a geometric estimation of the river's cross-sectional area is performed. This estimation leverages the filtered set of certain centroids, which represent high-confidence returns from submerged points across a lateral sweep. These centroids are spatially constrained between the detected left and right riverbanks and vertically below the estimated water surface, as determined from the sonar measurements.

The area computation is performed by constructing a polygon that approximates the submerged cross-sectional shape of the riverbed. The lower boundary of this polygon is formed by the ordered set of centroid coordinates, sorted by increasing scan angle to ensure continuity from the left bank to the right bank. The lateral limits of

the polygon are closed by projecting the leftmost and rightmost centroid segments to intersect with a baseline corresponding to a representative sonar depth. If an explicit intersection cannot be computed due to geometric parallelism, a fallback approximation is used by horizontally projecting the bank coordinates to the depth baseline.

Once the polygon is defined, its area is computed using Gauss's Area Formula, a numerical method for evaluating the area of an irregular polygon given its vertex coordinates.

$$A = \frac{1}{2}\left|\sum_{i=1}^{n}(x_i y_{i+1} - x_{i+1} y_i)\right|$$
$$\text{where} \quad (\mathrm{x}_{n+1}, y_{n+1}) = (x_1, y_1)$$

Figure 3.29: Gauss's Area Formula for Irregular Polygons

The result is a precise, unit-consistent estimate of the submerged cross-sectional area of a given stream's channel.

Chapter 4

Laboratory Experiments

4.1 Overview

The following chapter presents a series of controlled laboratory experiments designed to evaluate the performance of the StreamScope system and it's peripherals under various environmental conditions. The experiments primarily aim to assess the accuracy, reliability, and limitations of the laser rangefinder when subject to real-world factors such as solar radiation, water turbidity, and different substrate types.

Section 4.2 focuses on the laser's sensitivity to ambient solar radiation, examining how sunlight affects measurement reliability and signal quality. Section 4.3 investigates the laser's performance in increasingly turbid water, analyzing how suspended particles and differing bottom substrates such as sand and rock impact measurement accuracy. Additionally, effects of vertical displacement and water disturbances are explored. Section 4.4 evaluates the accuracy of the onboard accelerometer in calculating roll angles, a critical factor in estimating the true orientation of the scanning beam during a sweep.

Together, these experiments provide foundational validation for the sensor suite, inform the limits of its operation, and guide recommendations for field deployment and data interpretation.

4.2 Laser Performance Under Ambient Solar Radiation Conditions

4.2.1 Background

Laser range finders, especially those that are eye-safe and operate in the visible spectrum, are sensitive to ambient light interference. Egismos, the company that creates the laser range finder used in the StreamScope unit, details in the datasheet for the module that "measurement targets should avoid direct light exposure" [7]. Despite this, they do not explicitly say that the range finder can not be used in an outdoor setting during the day.

This experiment aims to determine the extent to which sunlight affects measurement accuracy and stability, and to identify operational limits or mitigation strategies for operation.

4.2.2 Methodology

To assess the impact of ambient solar radiation of Egismos laser rangefinder, a series of measurements were taken under varying sunlight conditions. The laser rangefinder was mounted to a plate facing downwards at 0° and attached to a tripod. A tub of water with a sandy bottom substrate was placed directly underneath to emulate scanning a shallow body of water. A pyranometer was used to record incident solar irradiance (W/m^2) at regular intervals throughout the trial. The pyranometer was mounted to the arm of the tripod.

In addition, an EXO2 Sonde was deployed in the water to monitor environmental conditions. This multi-parameter instrument is commonly used to measure variables such as turbidity, temperature, and specific conductance across a range of aquatic

environments. Although increasing turbidity was not an objective of this experiment, the instrument was used extensively throughout the turbidity experiments outlined in Section 4.3. Its readings are included to serve as a baseline for comparison in later experiments.



Figure 4.1: Solar Radiation Experiment Setup

The experiment was carried out on a mostly clear, sunny day, beginning during peak solar radiation hours. Laser measurements were recorded at fifteen-minute intervals, alongside concurrent pyranometer readings. To verify the accuracy of the pyranometer, its measurements were cross-referenced with solar radiation data provided by the National Weather Center in Norman, Oklahoma.



Figure 4.2: Verifying Water Height With Tape Measure

4.2.3 Results

The expected distance field was calculated by first measuring a reference distance with the laser to the bottom of the tub without water, then adjusting this value based on the eventually known water depth, using Snell's Law to account for the laser's refraction. The resulting measurement is the reading that is expected to be observed from the laser.

The turbidity measured by the EXO2 Sonde was approximately 2.9 Nephelometric Turbidity Units (NTU), indicating relatively clear water. For reference, the World Health Organization sets 5 NTU as the maximum allowable turbidity level for drinking water [13]. As expected, since no materials were introduced to intentionally increase turbidity during the experiment, the water remained consistently clear.

Table 4.1: Results from Solar Radiation Experiment - Table

Substrate Type	Sand
Measured distance between laser and bottom of tank (with tape measure)	1458 mm
Reference distance between laser and bottom of tank with substrate (with laser, without water)	1450 mm
Reference distance between laser and bottom of tank with substrate (with laser, with water)	1544 mm
Expected distance between laser and bottom of tank with substrate (with laser, with water)	1538 mm
Measured water depth in tank (with tape measure)	271 mm
Measured turbidity of water	2.9 NTU
Measured temperature of water	18.85 C

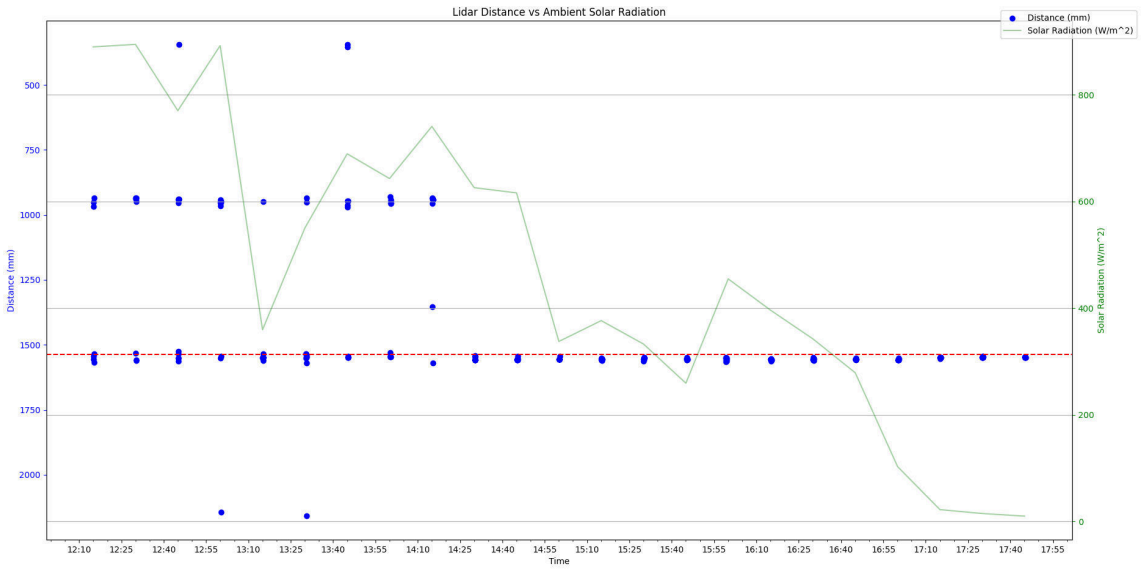

Figure 4.3: Results from Solar Radiation Experiment - Graph

4.2.4 Conclusions

Even under peak solar radiation conditions, the laser was generally able to record distance measurements close to the expected return value, demonstrating a reasonable level of robustness to ambient light interference. However, a small subset of the collected data showed outliers—distance readings that were clearly erroneous or implausible. These anomalies may have been caused by strong surface reflections, sensor saturation, or signal degradation due to direct sunlight entering the optical path.

Additionally, while the average distance measurements remained near the expected trend line, there was noticeably more variation in the spread of the points during periods of higher solar irradiance compared to those recorded under lower sunlight conditions. This increased variability suggests that while the laser can still perform adequately in bright environments when sampling at a high rate, measurement precision may suffer as ambient light intensity increases.

This observation highlights an important consideration for real-world deployment: although the laser remained functional in full daylight, its reliability and measurement accuracy improve noticeably under conditions of lower solar irradiance, such as during overcast weather or at times of day when sunlight is less direct. Knowing this, it is reasonable to conclude that the laser will produce its most accurate distance measurements during the night.

4.3 Laser Performance Under Increasing Turbidity

4.3.1 Background

As noted earlier in the context of airborne bathymetric LiDAR systems, turbidity—caused by suspended sediment, organic matter, and other particulates—can significantly degrade laser signal returns in aquatic environments [3]. This attenuation is especially problematic for systems that rely on clear optical paths, as increased scattering and absorption reduce the intensity and accuracy of reflected signals.

While some laser bathymetry systems mitigate this by using wavelengths like 532 nm (green), which experience lower absorption in water, even these systems are affected when turbidity levels are high. In submerged laser applications, where the laser must penetrate the water column and reflect off the bottom, turbidity presents a critical challenge to data reliability.

This section investigates how increasing turbidity levels affect the Egismos Laser Distance Module under controlled laboratory conditions. By gradually introducing particulate matter to simulate murkier water and observing how the laser system responds, this experiment helps define the operational limits of the device. Additionally, variables such as bottom substrate type, water depth, height above the water, and surface disturbances were included to understand how turbidity interacts with other environmental factors that also influence return accuracy.

4.3.2 Methodology

Similar to the solar radiation experiment, the laser module is fixed on a tripod facing downward at 0°. The bottom of the tub is then covered with the chosen bottom substrate, either sand or rock. For the experiments where sand is the bottom substrate,

varying levels of water were tested ranging from 120mm to 400mm to observe how turbidity influences returns at various water depths. To gradually increase the turbidity in the water, a Hi-Yield Horticultural Hydrated Lime was added in 1-2 gram increments (depending on the water's depth) every fifteen minutes and stirred to ensure proper dispersion. The EXO2 Sonde is situated near the center of the tub to measure turbidity and its sensor's submerged.



Figure 4.4: Turbidity Experiment Setup

Since the laser performs best under low solar radiation conditions and to more accurately quantify how turbidity affects the laser's distance returns, the experiments were conducted indoors where solar radiation is effectively zero. Each experiment was carried out until the laser's distance returns were considered "unusable", either if the laser began to capture the top of the water consistently or its measurements became too unstable to accurately quantify the distance to the bottom.

The Egismos laser distance module was polled every five seconds using it's single measurement mode, while the EXO2 sonde took turbidity measurements every second to ensure the data collected showed the changes to the retrievals over time with precision.

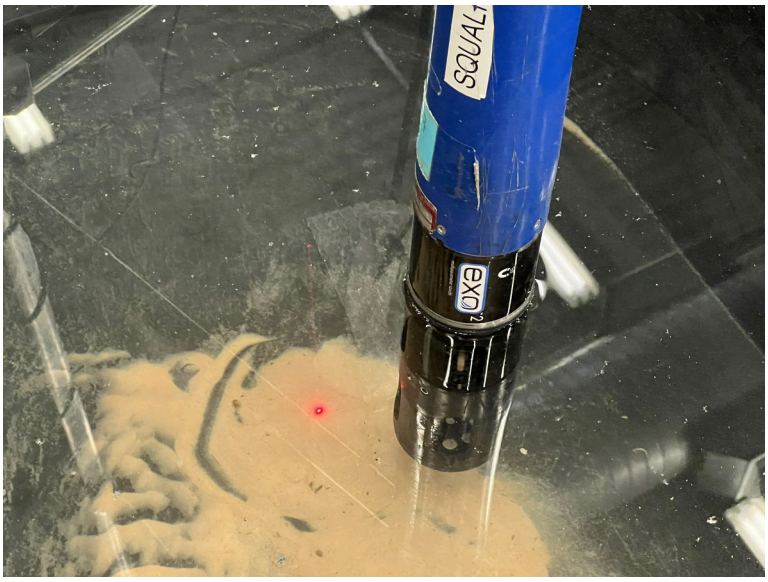

Figure 4.5: Laser and EXO Sonde Set-Up For Turbidity Experiment

4.3.2.1 Height Experiment

Most of the laboratory experiments were conducted from a relatively short distance from the laser to the water's surface. But, StreamScope is meant to be hung from trees and bridges, which are typically a little more than just a meter or two above the water's surface.

Because of this reason, a height experiment was conducted at a water depth of 350mm to verify the results that were captured from the other turbidity experiments can be applied when the distance between the laser and the water's surface increases.



Figure 4.6: Height Increase Turbidity Experiment Setup - Side View

The methodology for this experiment is identical to the other turbidity experiments, with the only exception being that the laser is now mounted on a ladder to increase the scanning distance to the bottom of the tub.

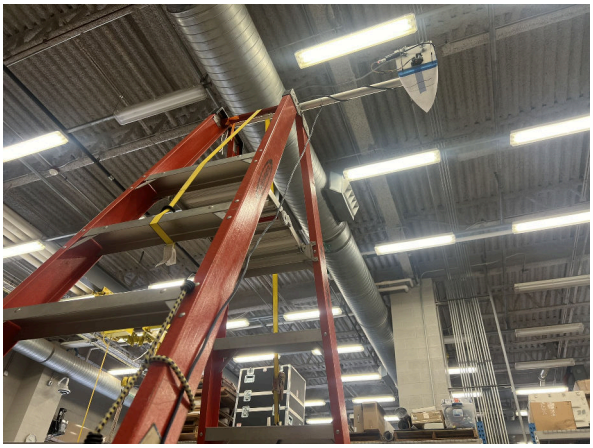

Figure 4.7: Height Increase Turbidity Experiment Setup - Upward View

4.3.3 Results

The following sections detail the results obtained by each turbidity experiment. The table for each experiment details important information, such as substrate type, reference distances, and expected laser return. It also details the estimated level of turbidity that affects laser retrievals, the point in which the laser's distance returns become too unstable or erroneous to be usable.

4.3.3.1 Bottom Substrate - Sand

Table 4.2: Turbidity Experiment Table - 120 mm Depth (Sand Bottom)

Substrate Type	Sand
Measured distance between laser and bottom of tank (with tape measure)	1450 mm
Reference distance between laser and bottom of tank with substrate (with laser, without water)	1450 mm
Reference distance between laser and bottom of tank with substrate (with laser, with water)	1488 mm
Expected distance between laser and bottom of tank with substrate (with laser, with water)	1490 mm
Measured water depth in tank (with tape measure)	125 mm
Estimated level of turbidity that affects distance retrievals	20 NTU
Measured temperature of water	22.26 C

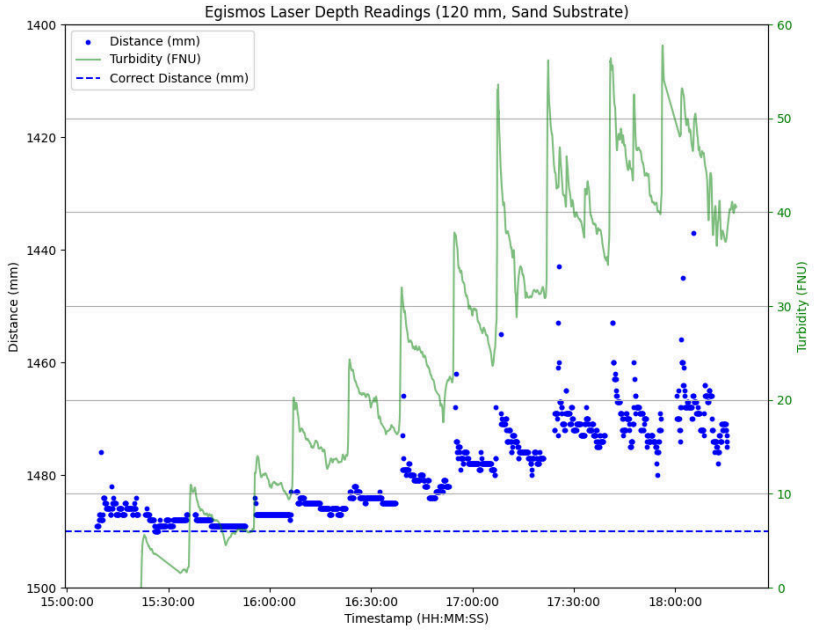

Figure 4.8: Turbidity Experiment Graph - 120 mm Depth (Sand Bottom)

Table 4.3: Turbidity Experiment Table - 150mm Depth (Sand Bottom)

Substrate Type	Sand
Measured distance between laser and bottom of tank (with tape measure)	1450 mm
Reference distance between laser and bottom of tank with substrate (with laser, without water)	1450 mm
Reference distance between laser and bottom of tank with substrate (with laser, with water)	1488 mm
Expected distance between laser and bottom of tank with substrate (with laser, with water)	1497 mm
Measured water depth in tank (with tape measure)	145 mm
Estimated level of turbidity that affects distance retrievals	18-20 NTU
Measured temperature of water	22.26 C

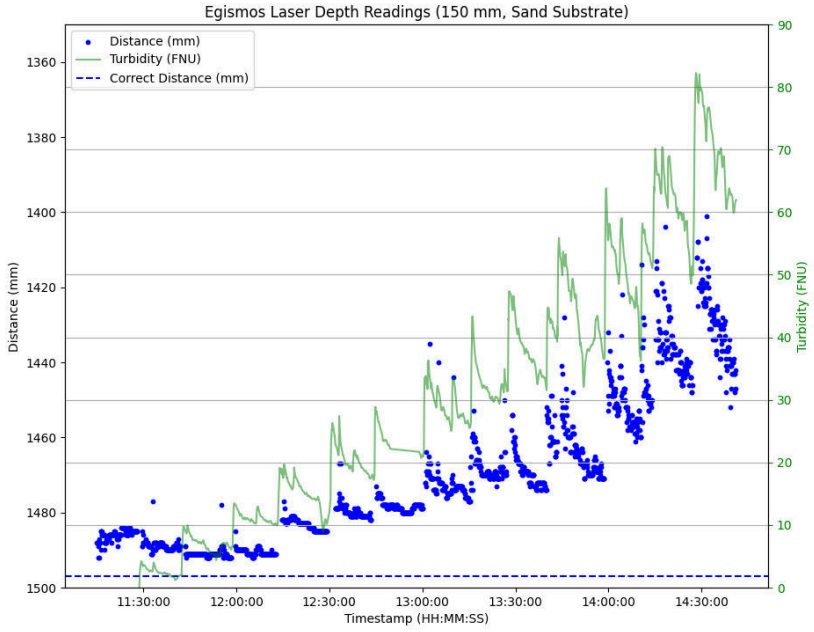

Figure 4.9: Turbidity Experiment Graph - 150mm Depth (Sand Bottom)

Table 4.4: Turbidity Experiment Table - 200mm Depth (Sand Bottom)

Substrate Type	Sand
Measured distance between laser and bottom of tank (with tape measure)	1450 mm
Reference distance between laser and bottom of tank with substrate (with laser, without water)	1450 mm
Reference distance between laser and bottom of tank with substrate (with laser, with water)	1506 mm
Expected distance between laser and bottom of tank with substrate (with laser, with water)	1515 mm
Measured water depth in tank (with tape measure)	200 mm
Estimated level of turbidity that affects distance retrievals	17-20 NTU
Measured temperature of water	22.1 C

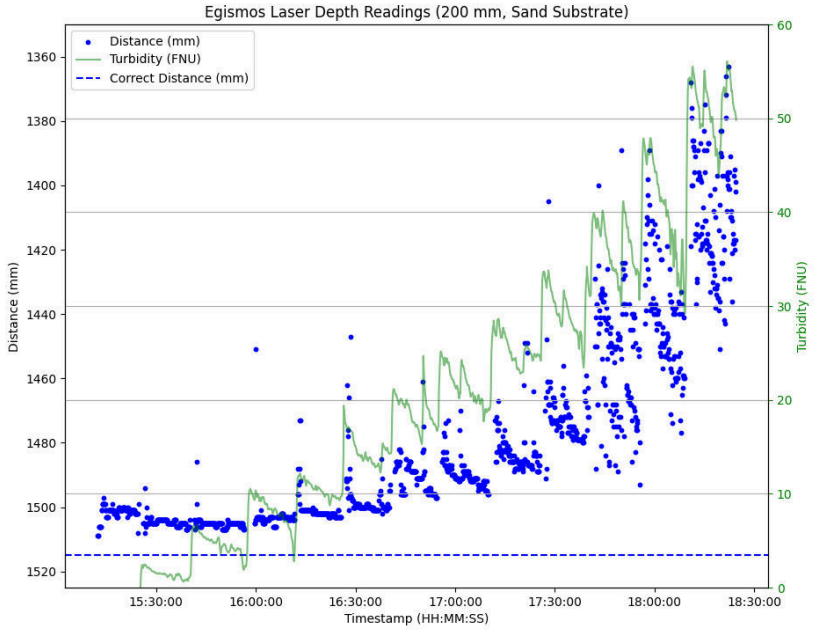

Figure 4.10: Turbidity Experiment Graph - 200mm Depth (Sand Bottom)

Table 4.5: Turbidity Experiment Table - 250mm Depth (Sand Bottom)

Substrate Type	Sand
Measured distance between laser and bottom of tank (with tape measure)	1450 mm
Reference distance between laser and bottom of tank with substrate (with laser, without water)	1450 mm
Reference distance between laser and bottom of tank with substrate (with laser, with water)	1529 mm
Expected distance between laser and bottom of tank with substrate (with laser, with water)	1529 mm
Measured water depth in tank (with tape measure)	245 mm
Estimated level of turbidity that affects distance retrievals	17-20 NTU
Measured temperature of water	22.4 C

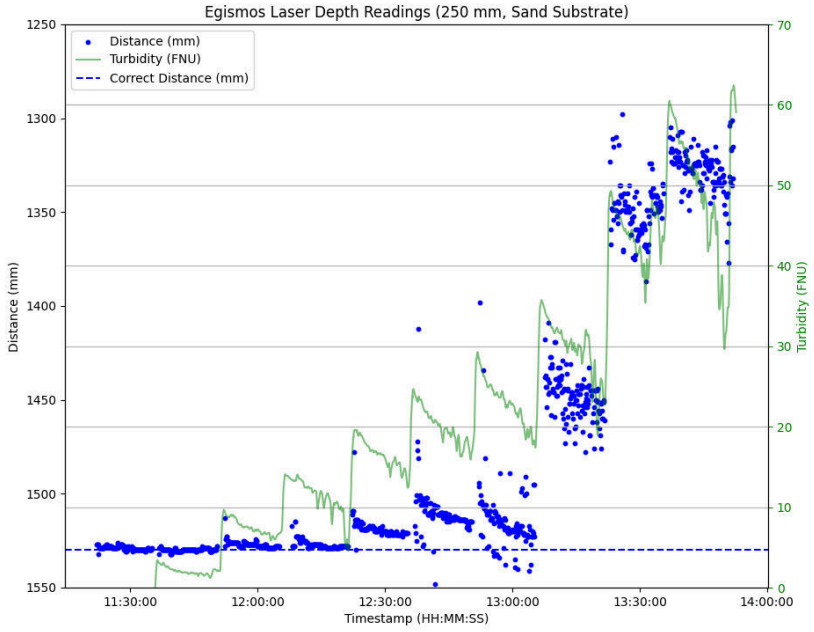

Figure 4.11: Turbidity Experiment Graph - 250mm Depth (Sand Bottom)

Table 4.6: Turbidity Experiment Table - 300mm Depth (Sand Bottom)

Substrate Type	Sand
Measured distance between laser and bottom of tank (with tape measure)	1450 mm
Reference distance between laser and bottom of tank with substrate (with laser, without water)	1450 mm
Reference distance between laser and bottom of tank with substrate (with laser, with water)	1557 mm
Expected distance between laser and bottom of tank with substrate (with laser, with water)	1551 mm
Measured water depth in tank (with tape measure)	310 mm
Estimated level of turbidity that affects distance retrievals	20-24 NTU
Measured temperature of water	22.2 C

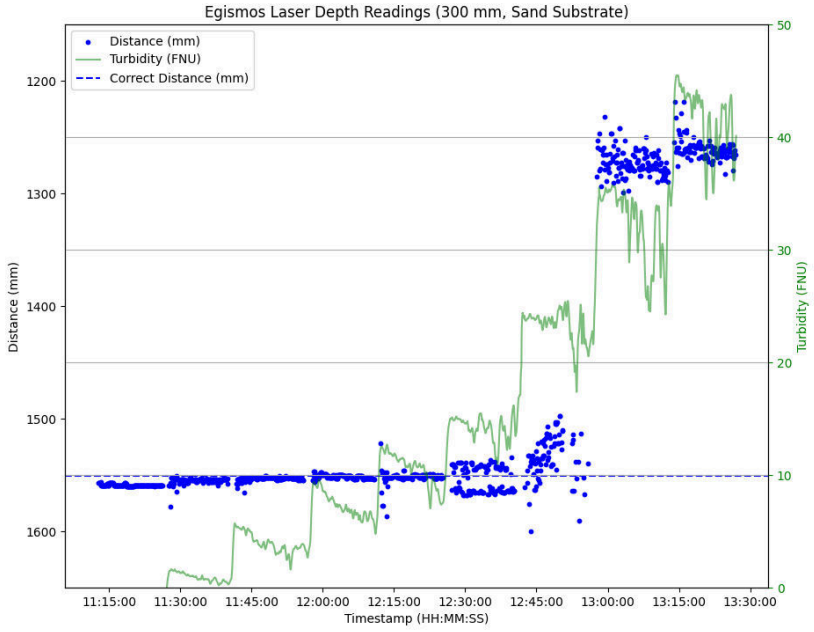

Figure 4.12: Turbidity Experiment Graph - 300mm Depth (Sand Bottom)

Table 4.7: Turbidity Experiment Table - 350mm Depth (Sand Bottom)

Substrate Type	Sand
Measured distance between laser and bottom of tank (with tape measure)	1450 mm
Reference distance between laser and bottom of tank with substrate (with laser, without water)	1450 mm
Reference distance between laser and bottom of tank with substrate (with laser, with water)	1571 mm
Expected distance between laser and bottom of tank with substrate (with laser, with water)	1564 mm
Measured water depth in tank (with tape measure)	350 mm
Estimated level of turbidity that affects distance retrievals	14-20 NTU
Measured temperature of water	22.4 C

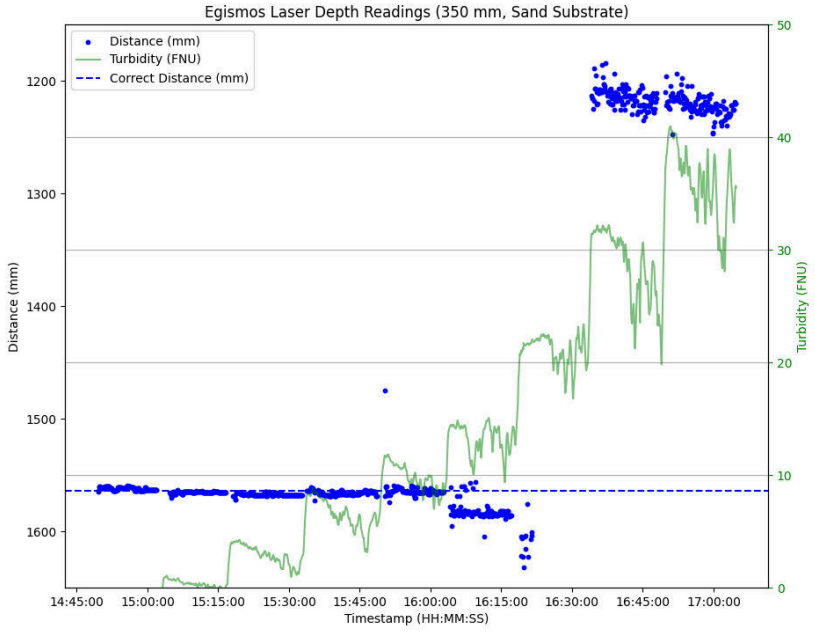

Figure 4.13: Turbidity Experiment Graph - 350mm Depth (Sand Bottom)

Table 4.8: Turbidity Experiment Table - 400mm Depth (Sand Bottom)

Substrate Type	Sand
Measured distance between laser and bottom of tank (with tape measure)	1450 mm
Reference distance between laser and bottom of tank with substrate (with laser, without water)	1450 mm
Reference distance between laser and bottom of tank with substrate (with laser, with water)	1589 mm
Expected distance between laser and bottom of tank with substrate (with laser, with water)	1580 mm
Measured water depth in tank (with tape measure)	400 mm
Estimated level of turbidity that affects distance retrievals	15-19 NTU
Measured temperature of water	22.4 C

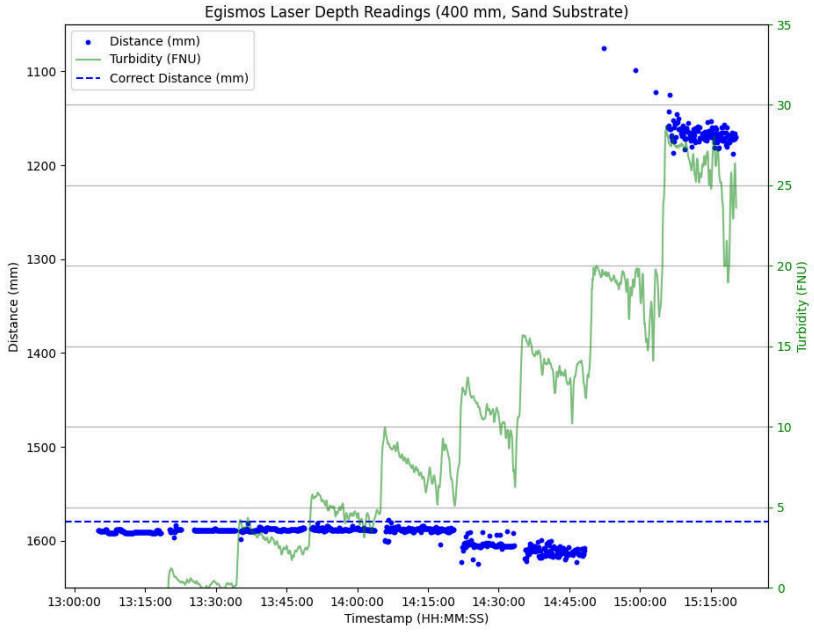

Figure 4.14: Turbidity Experiment Graph - 400mm Depth (Sand Bottom)

4.3.3.2 Bottom Substrate - Rock

Table 4.9: Turbidity Experiment Table - 350mm Depth (Rock Bottom)

Substrate Type	Sand
Measured distance between laser and bottom of tank (with tape measure)	1400 mm
Reference distance between laser and bottom of tank with substrate (with laser, without water)	1400 mm
Reference distance between laser and bottom of tank with substrate (with laser, with water)	1506 mm
Expected distance between laser and bottom of tank with substrate (with laser, with water)	1515 mm
Measured water depth in tank (with tape measure)	354 mm
Estimated level of turbidity that affects distance retrievals	17-25 NTU
Measured temperature of water	22.5 C

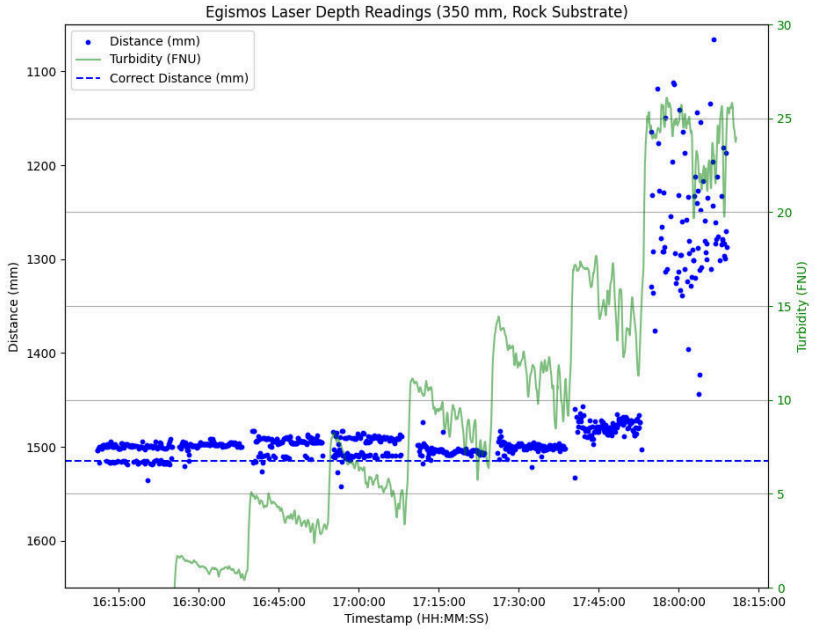

Figure 4.15: Turbidity Experiment Graph - 350mm Depth (Rock Bottom)

4.3.3.3 Height Increase

Table 4.10: Turbidity Experiment Table - 350mm Depth (Sand, Height Increase)

Substrate Type	Sand
Measured distance between laser and bottom of tank (with tape measure)	3260 mm
Reference distance between laser and bottom of tank with substrate (with laser, without water)	3247 mm
Reference distance between laser and bottom of tank with substrate (with laser, with water)	3393 mm
Expected distance between laser and bottom of tank with substrate (with laser, with water)	3373 mm
Measured water depth in tank (with tape measure)	349 mm
Estimated level of turbidity that affects distance retrievals	15 NTU
Measured temperature of water	23.5 C

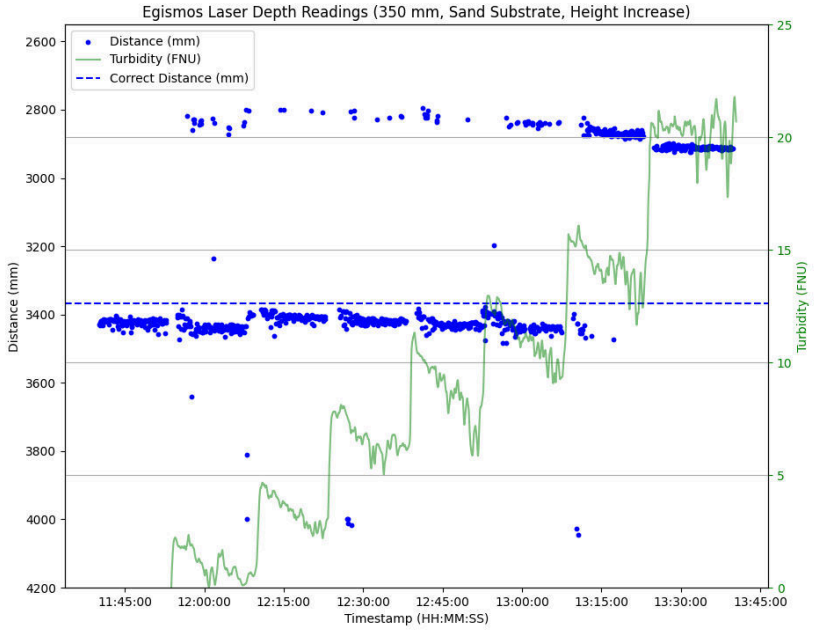

Figure 4.16: Turbidity Experiment Graph - 350mm Depth (Sand, Height Increase)

4.3.4 Discussion

Before discussing the results, it is important to define how turbidity is measured by the EXO2 Sonde.

From the EXO User Manual: "Turbidity is the indirect measurement of suspended solid concentration in water and is typically determined by shining a light beam into the sample solution and then measuring the light that is scattered off of the suspended particles" [15].

Because of the dynamic nature of water, turbidity can vary significantly throughout the water column and change rapidly as the water becomes mixed or as sediment settles. This is why when the hydrated lime is added every fifteen minutes, the turbidity jumps as it is mixed in, but smooths out as the lime dissolves. To maintain consistently rising turbidity levels throughout the experiment, lime was added at regular intervals, ensuring that suspended particle concentrations remain elevated.

In addition to this, the measurement process was never halted during the times when additional hydrated lime was added and stirred, contributing to some artifacts seen in the distance returns.

120, 150, and 200mm Turbidity Experiments (Sand)

These three experiments had largely the same result, both in the amount of turbidity required to deem the returns unusable and in the shape of the graph. It is important to note that the graphs for these experiments are incredibly granular on the y-axis, meaning that small visual differences between points are on the order of only a few millimeters. This was done to showcase the shape of the returns as turbidity increased.

When observing the returns as turbidity increases, these graphs produce an almost "wave" like appearance to them and the returns mimic those of the EXO2 Sonde for

turbidity. Knowing how the EXO2 Sonde measures turbidity with light, this isn't terribly surprising. But, what is intriguing is the laser's distance returns at this lower water depth being a proxy for turbidity. Being able to utilize a laser for non-contact turbidity measurements could greatly improve remote sensing capabilities. Unfortunately, since the Egismos laser distance module does not allow for users to see the light back scatter, it is not something that can be verified for this application.

The estimated amount of turbidity required to deem the distance returns unusable was around 20 NTU, According to the USGS, during base/low flow conditions, turbidity is usually observed to be around 10 NTU [16]. This means that the laser performed adequately throughout these experiments at lower depths.

250, 300, 350, and 400mm Turbidity Experiments (Sand)

At 250mm, we observe a different behavior when the turbidity reaches its "critical point" than the shorter depths before it. When the turbidity reaches around 15 NTU, it begins to do what the shorter depths exhibited, slowly forms into a "wave"-like function and becomes more unstable. But, as it increases between 15-20 NTU, it jumps to an intermediate location in the water column, which was not something that was observed before. At this point, the distance returns become unusable. After this occurs, though, it jumps up again and begins to only return the distance to the surface of the water.

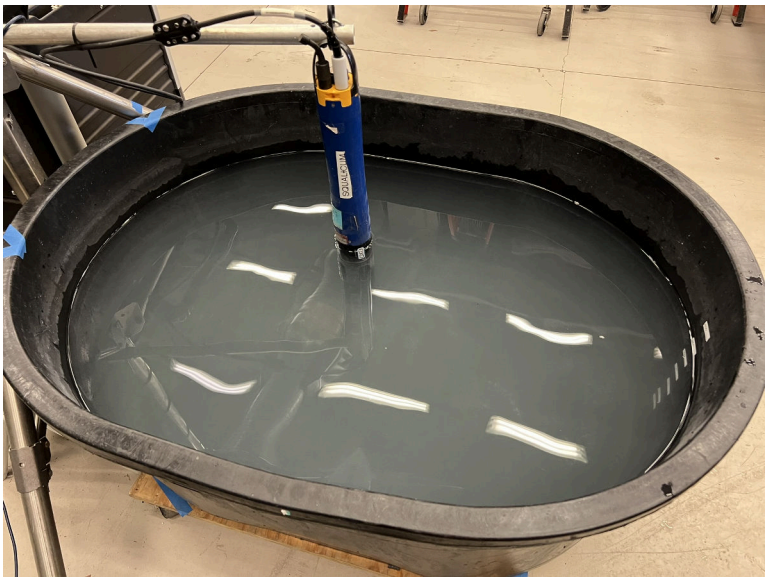

Figure 4.17: Turbid Water During Turbidity Experiments

Regarding the rest of the depths, the jump to the surface when the turbidity approaches and exceeds 20 NTU is also observed, but they do not exhibit the same intermediary jump that the measurements at 250mm exhibit or the "wave"-like effect. Instead, the Egismos laser distance module began to throw an error, unable to return any values which is why there is a gap between measurements. After the turbidity reaches around 30 NTU, the distance returns begin again with all the returns centered around the water's surface.

350mm Turbidity Experiment (Rock)

The 350mm experiment using a rock as the bottom substrate yielded similar to results to the 350mm experiment over sand, with only a few differences. Stable distance returns when turbidity was low exhibited two very distinct clusters that were separated by a few millimeters, which was not seen when the experiment was carried out with sand as the bottom substrate. Despite this, the measurements remained usable and

accurate until the 15-20 NTU range, where retrievals became unusable, with some being near the surface of the water.

350mm Turbidity Experiment With Height Increase (Sand)

When the height was increased from the previous height used for the other turbidity experiments, a few new responses were observed. Even when the turbidity was rather low, there were a few distance returns from the top of the water, but only a few. As the turbidity approached between 15 NTU and beyond, the returns briefly became inconsistent and then strictly originate from the surface of the water, which is a slightly lower threshold for the returns to become unusable than the prior experiments.

In addition to this, it is important to note during the experiment that the Egismos laser distance module returned its first observed "WEAK SIGNAL" measurement, which is different than the other experiments where the turbidity in the water column caused the sensor to send a basic error message.

Conclusions

Throughout all of the experiments, one could generally expect that the laser would be able to retrieve a usable depth measurement if the human observers could see the bottom of the tub themselves. In the experiments only a meter or so above the water's surface, this expectation was actually exceeded, where there were numerous occasions where the laser retrieved the distance to the bottom of the tub.

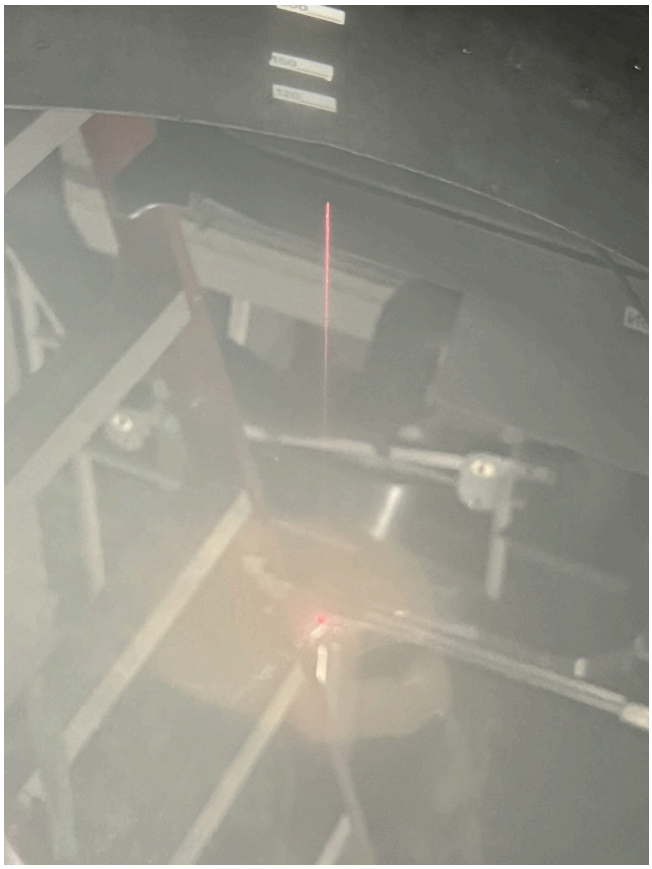

Figure 4.18: Egismos Scanning Through Turbid Water

Most of the measurements began to become inconsistent or result in surface retrievals around 20 NTU, while the experiments at an increased height exhibited the same behavior at around 15 NTU. Despite this difference, both are still above the 10 NTU conditions during base flow established by the USGS, making the laser viable for StreamScope's application.

Informal Test of Egismos Measurement Modes

All of the above experiments were conducted when the primary way of polling the Egismos laser distance module was in single measurement mode. When StreamScope

was first assembled, continuous measurement mode was tested and observed to see if the results of the original, height-adjusted, 350mm experiment with sand as its bottom substrate would be affected by a different mode. By this time, the EXO2 Sonde was past its viable calibration date and making an order for the solutions to recalibrate it was not possible, so turbidity measurements were ommitted as a result. Shown below is a graph of the original 350mm experiment using single measurement mode and the test carried out by StreamScope using continuous measurement mode with their times normalized. Since the same amount of lime was added and all other experimental conditions were kept consistent, the turbidity readings from the original 350mm experiment serve as a valid baseline for comparison with the continuous measurement test. StreamScope sent its measurements in batches of five, so multiple measurements appear at singular timestamps



Figure 4.19: Single Measurement vs Continuous Measurement Mode

While there are no scientific conclusions that can be drawn from this comparison and test, the returns seemed to be more consistent and perform better in higher turbidity conditions than when the experiment was conducted in single measurement mode.

Because of this, the decision to operate the Egismos in continuous mode as its default mode was made.

4.4 Accelerometer Accuracy for Angle Calculation

4.4.1 Background

To verify the accuracy of the accelerometer selected for angle estimation, a simple test was performed. In field deployments, the StreamScope hangs above a stream, and minor deviations from vertical can cause the servo's reported angle to diverge from the actual angle of the laser beam. Since the system uses a low-cost accelerometer instead of a full IMU, this experiment aims to validate whether the accelerometer provides sufficient accuracy for correcting such deviations.

4.4.2 Methodology

The laser unit was positioned at a fixed height above a level surface and tilted incrementally. For each tilt, the actual angle of the laser was calculated using inverse cosine, based on the measured hypotenuse (laser path length) and vertical offset from the sensor to the ground. These reference angles were compared to angles calculated from the accelerometer.

Each test was repeated every 3 degrees from -40 to 40 degrees based on the direct servo angle input. The difference between the reference angle and the accelerometer reading was recorded.

4.4.3 Results

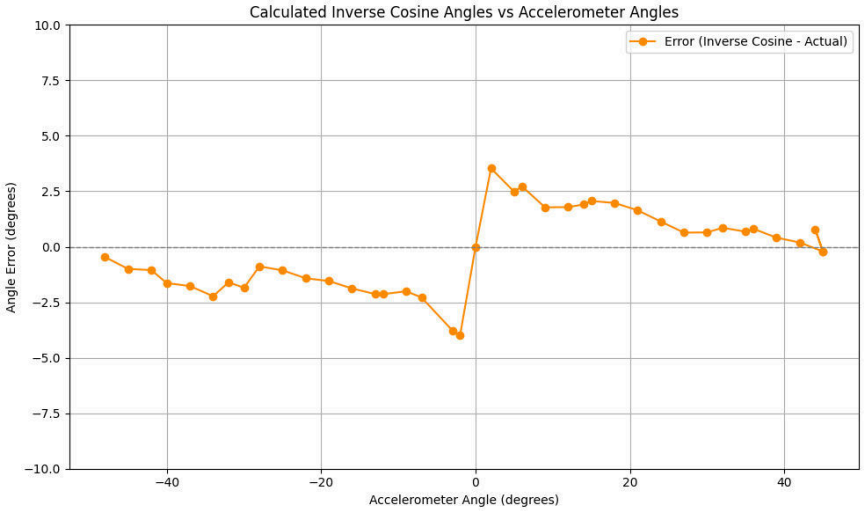

Figure 4.20: Error Between Calculated Angle and Accelerometer Angle

4.4.4 Conclusion

The accelerometer showed acceptable accuracy across the range of tested angles. Accuracy improved at higher tilts—where precise angular correction is most beneficial. While measurements near nadir were less accurate due to the nature of the gravity vector, these errors are not problematic in practice. At small incidence angles (e.g., 4°), Snell's Law has minimal impact on the refracted path of the laser beam, so slight angular discrepancies do not meaningfully affect the calculated distances. This validates the accelerometer as a sufficient, low-cost solution for estimating tilt in the deployed scanning system.

Chapter 5

Field Deployment

5.1 Overview

The StreamScope system was designed to provide an autonomous, solar-powered solution for non-contact stream monitoring through laser-based cross-sectional scanning. After iterative prototyping and refinement, the system was field-tested in a real-world environment to validate its performance under natural conditions. This deployment took place at Falls Creek in Davis, Oklahoma—an ideal testbed due to its variable flow conditions and prior surveying by the United States Geological Survey (USGS). The field deployment served as the first full integration of the StreamScope's hardware, software, and scanning methodology in situ. The objective was to evaluate the accuracy, robustness, and reliability of the system, as well as to directly compare its results with a professional total station survey conducted by USGS.

5.2 Description of Setting

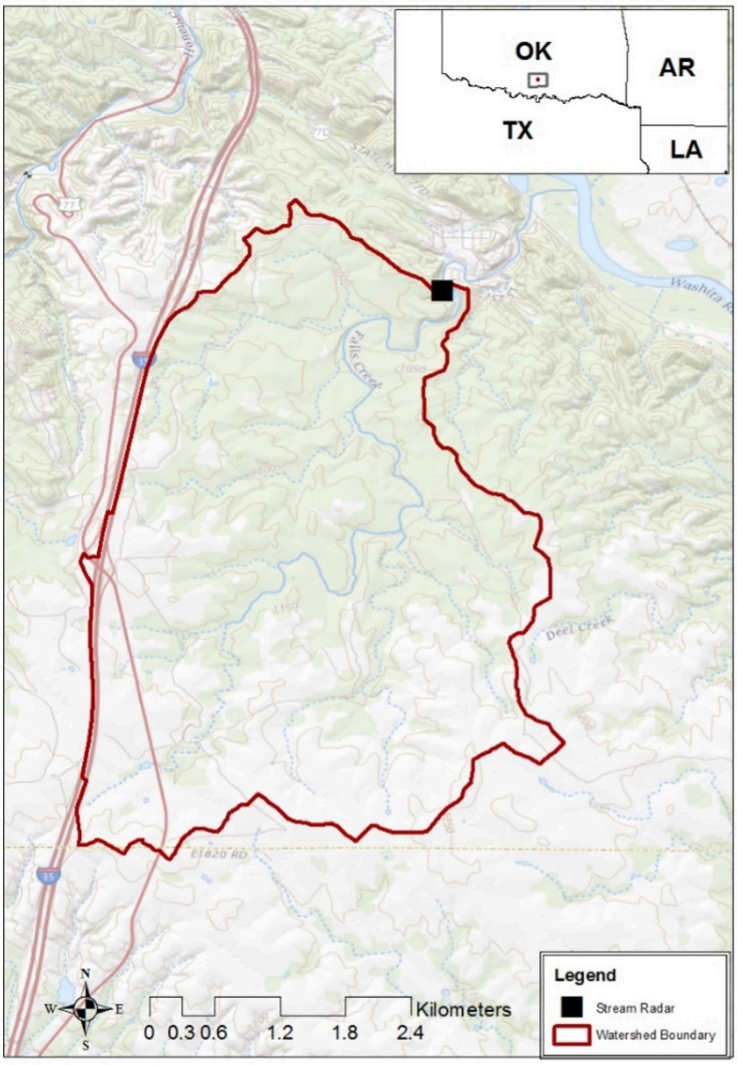

Figure 5.1: Falls Creek - Davis, OK

Falls Creek, located in Davis, Oklahoma, was selected as the deployment site for the StreamScope system based on a combination of practical and environmental considerations. The creek flows through a naturally carved channel with distinct bank features, moderate width, and a combination of shallow and turbulent water sections—conditions well-suited for evaluating a non-contact scanning system like StreamScope. The site lies within a 15.1 km^2 catchment area characterized by mixed terrain

and variable streamflow, providing a realistic and dynamic test environment for autonomous surface water monitoring.



Figure 5.2: Panoramic View of Falls Creek near Davis, OK

The site offered several advantages for deployment:

- **Accessibility:** Falls Creek is easily accessible by vehicle and foot, allowing for straightforward transportation and setup of equipment, as well as follow-up maintenance or troubleshooting.
- **Varied Flow Conditions:** The creek exhibits both calm and turbulent flow regions, enabling the system to be tested across different hydrodynamic scenarios within a single location.
- **Solar Exposure:** The surrounding area provided ample sunlight for consistent solar charging, critical for validating StreamScope's ability to operate autonomously over extended periods.
- **Prior Survey Data:** A professionally conducted total station survey by the United States Geological Survey (USGS) was previously carried out at this location. This allowed for a meaningful comparison between StreamScope's laser-derived cross-sections and ground-truth data.

The selected site thus represented a realistic environment for validating the end-to-end functionality of StreamScope, from scanning and data collection to solar-powered operation and eventual data retrieval.

5.3 Deployment Configuration

The core deployment setup included a solar power system, waterproof electronics housing, and a Raspberry Pi-based control system responsible for data acquisition and communication.

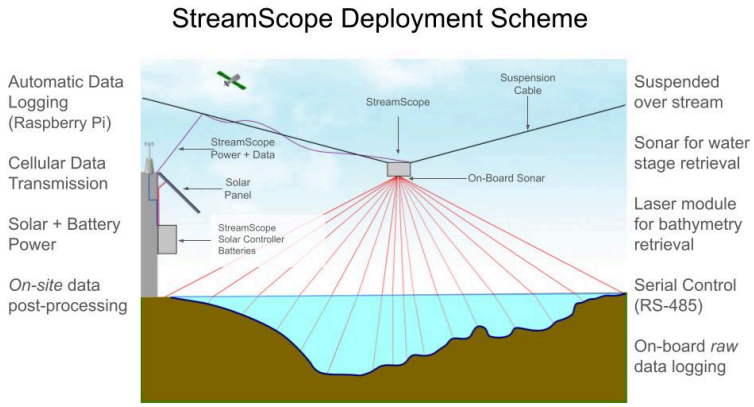

Figure 5.3: Deployment Scheme Diagram

A compact solar panel powered the system, charging two 12V batteries within a waterproof, weather-resistant enclosure. This ensured uninterrupted operation in remote, off-grid conditions. The enclosure also protected the control electronics from moisture, debris, and temperature fluctuations.



Figure 5.4: Enclosures and Solar Panel at Falls Creek near Davis, OK

At the heart of the system was a Raspberry Pi, configured to manage all automation and communication tasks. Using the built-in `cron` scheduler, the Raspberry Pi executed a Python script at regular intervals to poll the StreamScope unit for measurement data via serial communication. This script also handled timestamping, data formatting, and basic error handling to ensure reliable data capture.

```
# Push output file to server via SFTP
srv = pysftp.Connection(host=static_ip, username="NotStreamScope",
    password="NotThePassword")
try:
    with srv.cd("data/fallscreek"):
        srv.put(file_name)
    srv.close()
    logging.info(success_message)
except e:
    logging.error(e)
```

Figure 5.5: StreamScope Deployment Script Sending Data to Remote Server

In addition to local data logging, the Raspberry Pi was programmed to transmit collected data to a remote server via an available network connection. This allowed for real-time access to measurement results and provided redundancy in case of local storage failure. The ability to monitor system performance and retrieve data remotely was a key step toward enabling long-term, unattended deployments in field environments.

Together, this configuration allowed StreamScope to function as a self-sufficient, solar-powered monitoring station—capable of collecting, storing, and transmitting high-resolution cross-sectional data of flowing water in a completely automated fashion



Figure 5.6: StreamScope Deployed at Falls Creek near Davis, OK

5.4 Scanning Setup and Strategy

The deployment site at Falls Creek presented favorable conditions for remote scanning, with no significant constraints on power availability or data transmission. As a result, the StreamScope system was configured to operate at full scanning capacity, enabling high-resolution cross-sectional profiling at regular intervals.

The following parameters were used for each scanning cycle:

- **Measurement Type:** Full angular sweep from $-50°$ to $50°$, in increments of $1°$, covering a $100°$ field of view across the stream.
- **Samples per Angle:** 30 individual distance measurements were taken at each angular position to reduce noise and increase measurement reliability
- **Scan Interval:** Measurements were triggered automatically every 30 minutes using a scheduled `cron` job on the Raspberry Pi.

This strategy allowed StreamScope to generate dense, repeatable point clouds representing the cross-sectional profile of the creek channel. The scanning routine was designed to balance measurement resolution and data volume, while accommodating the variability of natural stream environments. While StreamScope scanned every 30 minutes, the only cross-sections that were examined were those taken during nighttime.

5.5 Retrieval of Cross-Sections



Figure 5.7: Laser Beam Path During a Sweep

When StreamScope was first deployed, the stream channel had turbulent conditions along the left bank, causing interesting behavior. This was shown as erroneous clusters of measurements that were evenly spaced vertically in Fig. 5.7.

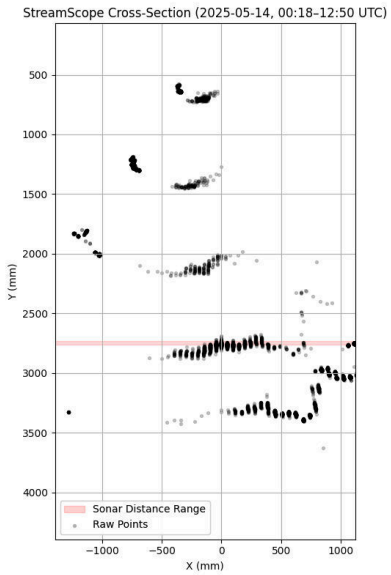

Figure 5.8: Erroneous Returns Early in Deployment

While a definitive explanation could not be verified, it is likely related to the behavior of the Egismos laser rangefinder, which uses a phase-shift measurement technique to determine distances.

Phase-shift laser rangefinders work by emitting a modulated laser signal and measuring the phase difference between the emitted and reflected waves. This phase difference corresponds to a time delay and is used to calculate distance. However, under turbulent flow conditions—such as those observed along the left bank during early deployment—rapid surface disturbances, bubbles, and splashing can create multiple reflective surfaces at varying depths. These include the air–water interface, suspended droplets, and even sub-surface reflections from foam or turbidity.

Such dynamic and inconsistent surfaces can introduce multiple return signals with different phase offsets. When the phase unwrapping or signal interpretation algorithm misidentifies which return is valid, the system may incorrectly register several plausible distances at the same angle. This can result in evenly spaced vertical clusters in the data, reflecting ambiguous phase returns rather than true physical structure.

Despite this, due to the sheer number of measurements taken at each angle and the post-processing algorithms utilized, a cross-section can be interpreted. And, as the water's current subsided, the picture of the stream's cross-section becomes even more accurate.



Figure 5.9: Turbulent Water at Falls Creek near Davis, OK

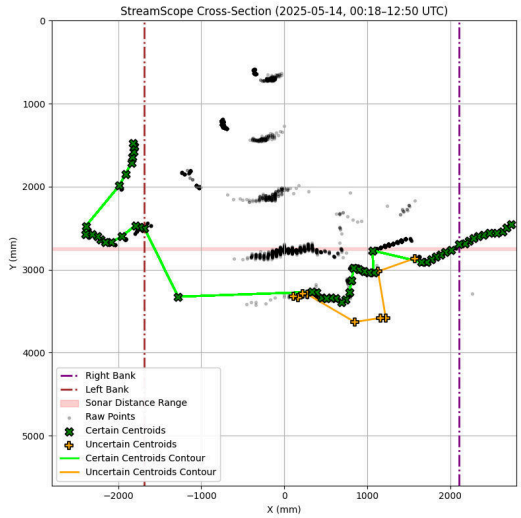

(a) May 14th, 2025

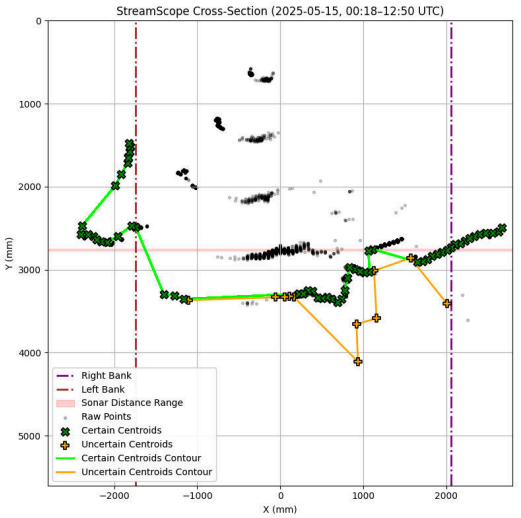

(b) May 15th, 2025

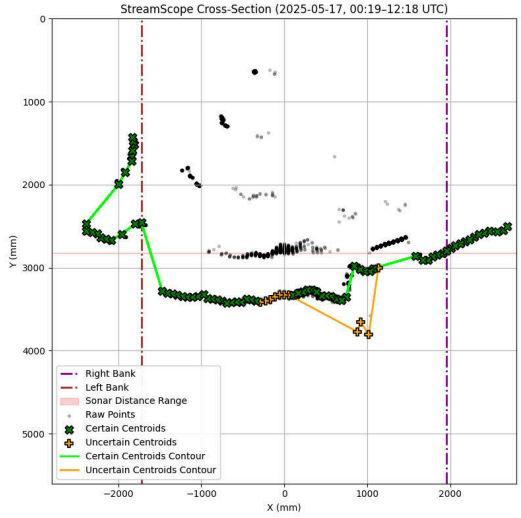

(c) May 17th, 2025

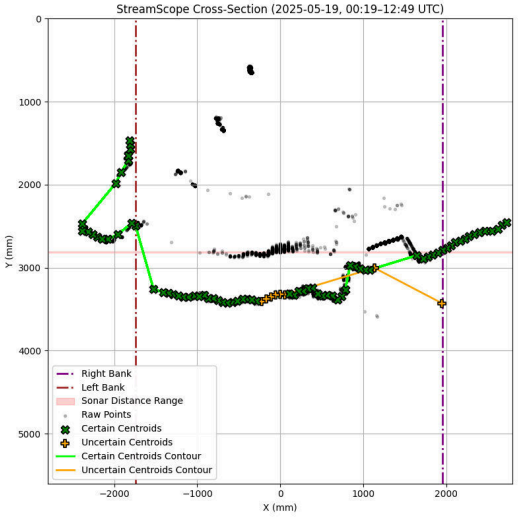

(d) May 19th, 2025

Figure 5.10: StreamScope Cross-Sections (05/14 - 05/19)

Although early measurements exhibited artifacts due to turbulent surface conditions, the high volume of data collected by StreamScope ultimately enabled reliable cross-sectional reconstruction. With each scan producing hundreds of data points and scans scheduled at regular intervals, the system generated a dense dataset. This made

it possible to distinguish consistent structural features of the stream channel from transient noise caused by splashing, foam, or sensor misreads.

Through post-processing—including the application of the previously discussed 2D KDE method—it was possible to extract the most probable cross-sectional profile from the raw measurements. KDE proved especially valuable in emphasizing stable return regions while de-emphasizing scattered or inconsistent readings. As a result, even though early data included significant noise, a coherent and representative stream cross-section was successfully recovered, demonstrating the robustness of the sensing and analysis pipeline in real-world conditions.

5.6 Comparison to Total Station Survey Conducted by the United States Geological Survey

To evaluate the accuracy and effectiveness of the StreamScope system, its generated cross-sections were compared against a ground-truth total station survey conducted by the United States Geological Survey (USGS) at the same site. The total station data serve as a highly trusted benchmark, acquired through precise manual measurement techniques under controlled conditions. This comparison represents a critical validation step for StreamScope, providing a means to assess its real-world performance against industry-standard methods. It is important to note that minor discrepancies may arise due to slight offsets between the exact locations of StreamScope's cross-section and the surveyed total station measurements. These spatial differences can affect direct point-to-point comparisons but do not diminish the overall validity of the assessment.



Figure 5.11: USGS Total Station Survey at Falls Creek near Davis, OK

The results demonstrate a high degree of alignment between the StreamScope-generated cross-section and the USGS survey. Key channel features—including bank locations, overall width, and streambed curvature—were accurately captured by StreamScope. Despite being a non-contact, autonomous system operating under ambient and sometimes turbulent environmental conditions, StreamScope was able to replicate the primary geometric profile of the channel with remarkable precision.

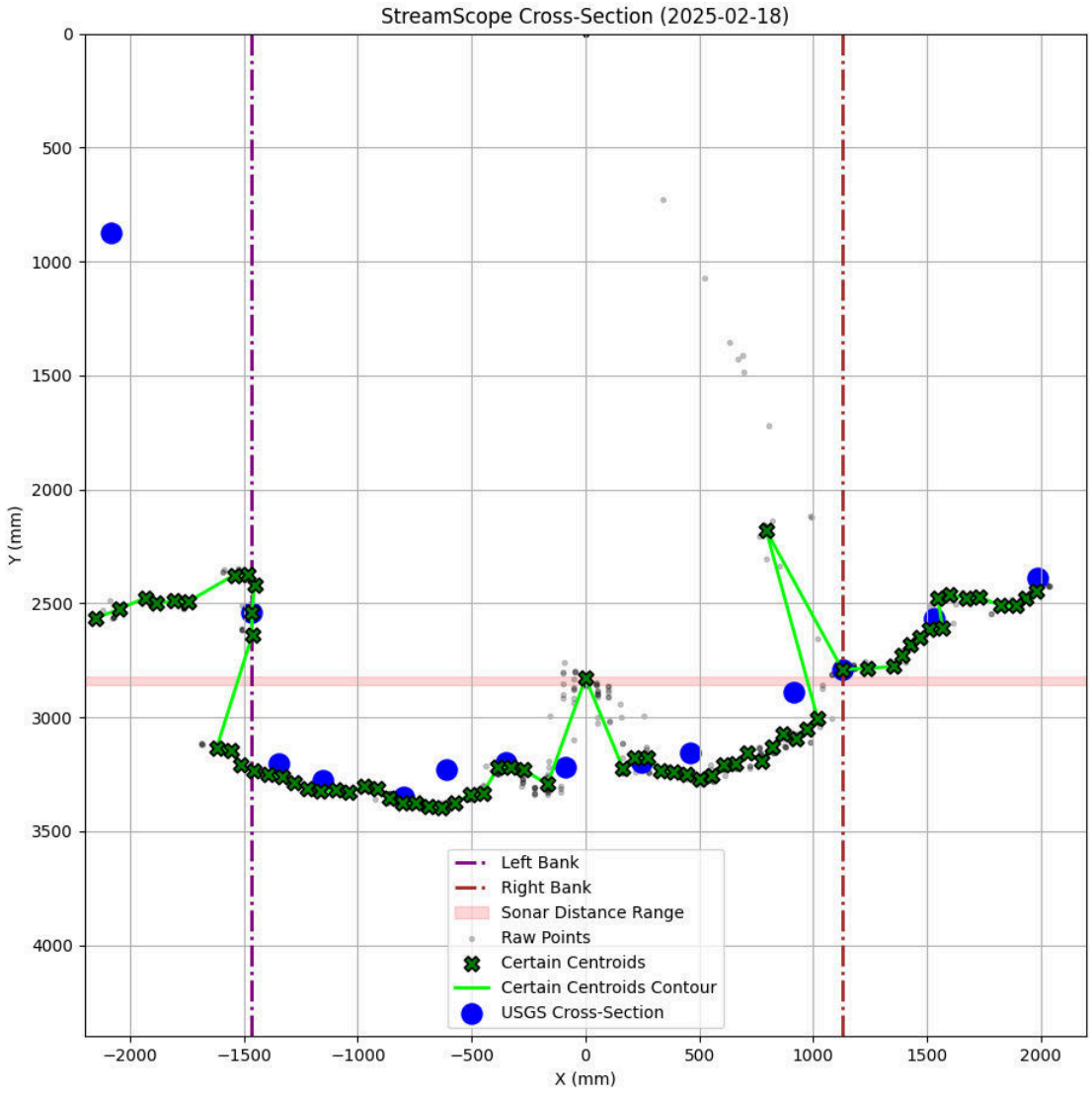

Figure 5.12: StreamScope Cross-Section Compared to the USGS Cross-Section

Moreover, the StreamScope system offered significantly higher spatial fidelity than the total station survey, especially across the channel. While total station points were manually spaced and necessarily limited in resolution, StreamScope provided dense, continuous sampling across the entire scan width, offering a richer depiction of fine-scale channel variability. This high-resolution capability is particularly valuable in capturing

dynamic or transitional features, such as subtle bank slopes, small-scale bedforms, or flow-induced surface anomalies, that may be underrepresented in traditional surveys.

The success of this comparison validates the core objectives of StreamScope: to design a low-cost, autonomous, and deployable sensor system capable of producing scientifically credible stream cross-section data. The ability to closely match the USGS benchmark—while simultaneously offering improved measurement density and requiring no human operation—demonstrates the potential of StreamScope to serve as a viable alternative or complement to conventional surveying techniques, especially in remote, hazardous, or frequently changing environments.

This convergence of agreement with gold-standard measurements and the advantages of automation, scalability, and resolution marks the culmination of the StreamScope system's development. It establishes a strong foundation for future deployments and further refinements in autonomous stream monitoring technologies.

Chapter 6

Conclusions

6.1 Summary of Work

This thesis presented the development, evaluation, and field validation of StreamScope, a novel, low-cost, fixed-mount laser scanning system designed for high-resolution stream bathymetry in shallow rivers with dynamic geomorphologies. Motivated by the limitations of conventional surveying techniques—such as Total Station surveys, airborne LiDAR, and photogrammetry—StreamScope offers an autonomous, non-contact solution suitable for continuous monitoring in remote or hazardous environments.

The system integrates a Class II 620 nm laser rangefinder, a high-resolution sonar sensor, an inclinometer, and a waterproof servo, all managed by a Teensy 4.1 microcontroller. The firmware employs Modbus RS-485 for robust communication, supports multiple scanning modes, and includes onboard datalogging to SD card. Power-efficient design choices, modular PCBs, and robust environmental protection measures (including PETG 3D-printed components and waterproof enclosures) enable long-term solar-powered deployment.

Laboratory tests established the sensor's performance boundaries under variable lighting, turbidity, substrate types, and water depths. StreamScope demonstrated functionality in turbidity levels up to 20 NTU and under varying heights and solar

conditions. Field deployments at Falls Creek, OK validated its performance in a real-world setting, with results closely matching those of a USGS-conducted Total Station survey while offering vastly improved temporal resolution and spatial fidelity.

A custom post-processing pipeline converted raw measurements into corrected Cartesian coordinates using Snell's Law and employed kernel density estimation to extract meaningful cross-sectional profiles and centroids. These outputs enabled the generation of dynamic stage–area ratings crucial for accurate and remote streamflow estimation.

6.2 Contributions

The core contributions of this thesis include:

- A fully operational prototype of a fixed-mount laser scanning system for real-time, remote stream monitoring, built using low-cost and off-the-shelf components.
- A robust design methodology encompassing sensor selection, mechanical and PCB design, firmware architecture, and integration strategies tailored to USGS requirements.
- A novel scanning and post-processing pipeline, including the use of 2D Kernel Density Estimation for centroid estimation and the application of Snell's Law for submerged coordinate correction.
- Empirical evidence from laboratory and field trials demonstrating the feasibility and accuracy of using a Class II red laser for stream bathymetry, even in moderately turbid conditions.
- Successful integration with existing USGS workflows and dataloggers, supporting both Modbus RTU communication and autonomous operation via pre-configured sweeps and register control.

These innovations provide a foundation for accessible, scalable, and continuous stream monitoring in environments previously underserved by existing surveying methods.

6.3 Future Work

6.3.1 Enhanced Laser Range Finder with Signal Access

The current StreamScope system uses a commercial red laser rangefinder that provides only distance readings, limiting the ability to assess signal quality or apply adaptive filtering to improve accuracy in challenging conditions like turbidity or surface turbulence.

To overcome these limitations, an in-house laser rangefinder prototype was explored during development. The design utilized a green laser diode and a custom detection circuit, aiming to provide full access to raw return signals and allow for tunable signal processing tailored to aquatic environments.

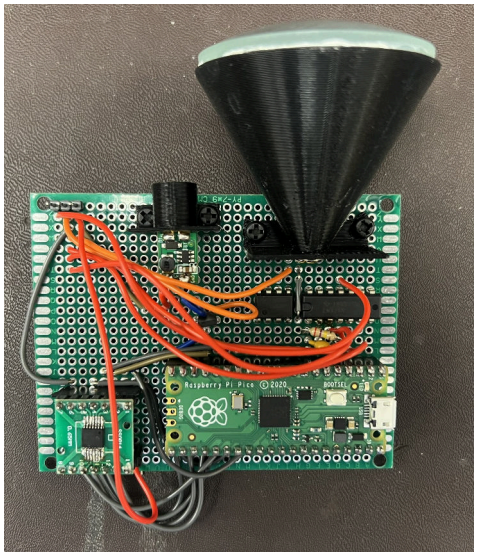

Figure 6.1: Prototype Green Laser Range Finder

While initial testing showed potential, the in-house laser system was ultimately set aside due to time constraints. Completing the full integration, calibration, and signal processing workflow required more development time than the project schedule allowed. As a result, focus shifted to finalizing the production-ready system using the Egismos module to ensure timely field deployment and validation.

Despite being shelved, this in-house effort provides a foundation for future versions of StreamScope. A custom laser system with raw signal access could significantly enhance measurement fidelity, enable deeper analysis of the return environment, and open the door to novel applications such as turbidity estimation or confidence scoring per data point.

6.3.2 Self-Sufficient StreamScope

While the current deployment model relies on external dataloggers (e.g., USGS Sutron Satlink3) for scheduling, triggering, and communication, making StreamScope more autonomous would simplify deployment and broaden its applicability. Possible enhancements include:

- Integrated cellular or satellite communication, removing dependence on external logging infrastructure and allowing true plug-and-play deployment in remote locations.
- Environmental feedback-driven scanning, where StreamScope could adapt its scanning rate or resolution based on stream conditions, battery level, or event detection (e.g., sudden turbidity increase or storm events).
- Redundant sensors for error-checking and self-diagnosis, improving system resilience and alerting operators to issues in real time.

6.3.3 Adaptive Post-Processing Techniques

While the current post-processing pipeline—based on geometric filtering, Snell's Law correction, and 2D Kernel Density Estimation—yields reliable cross-sections, it still relies heavily on manually tuned thresholds and fixed rules. In dynamic stream environments where water clarity, surface turbulence, and flow conditions fluctuate rapidly, these static filters may be insufficient to handle all error cases effectively.

To address this, machine learning techniques represent a promising direction for future improvements. Specifically, supervised or semi-supervised learning models could be trained to:

- Adaptively prune noisy measurements based on patterns learned from historical scans, rather than relying on fixed range, angle, or deviation cutoffs.
- Infer missing or obstructed scan data by learning the typical cross-sectional structure of the site over time, using adjacent angles, past sweeps, and surrounding return behavior to reconstruct likely channel geometry.

For example, a lightweight neural network or decision tree ensemble could be trained on labeled field and laboratory data to distinguish valid submerged returns from outliers. Alternatively, sequence-based models (e.g., temporal convolutional networks) could leverage the temporal structure of sweeps to predict how a cross-section evolves over time, making it possible to interpolate across partial or failed scans.

Such techniques would not only improve measurement accuracy but also enhance automation, enabling real-time anomaly detection, automated scan validation, and dynamic confidence scoring for each returned point. This would be especially beneficial in remote deployments where manual inspection of scan logs is impractical.

Future work may explore:

- Building a dataset of labeled laser returns under varying turbidity, flow, and lighting conditions for training and evaluation.
- Comparing traditional filtering techniques (e.g., outlier rejection, low-pass smoothing) against ML-based approaches in terms of accuracy and computational cost.
- Deploying lightweight models on-device or at the server level to support real-time filtering and automated alerts.

By integrating machine learning into the post-processing pipeline, StreamScope can evolve from a purely measurement-driven instrument to a data-smart platform capable of learning from its environment and improving over time.

Bibliography

[1] Trimble Inc., *Trimble SX12 Scanning Total Station Datasheet*, 2021. Available: https://trl.trimble.com/docushare/dsweb/Get/Document-966562/Datasheet%20-%20Trimble%20SX12%20Scanning%20Total%20Station%20-%20English%20(US)%20-%20Screen.pdf

[2] U.S. Geological Survey, "Setting and Configuring a Total Station, Version 1.0 — Southeast Coast Network Standard," 2021. https://irma.nps.gov/DataStore/DownloadFile/605809

[3] Kinzel, P. J., et al., "Bathymetric Structure from Motion: Extracting Shallow Stream Bathymetry from Multi-View Stereo Photogrammetry," *J. Am. Water Resour. Assoc.*, 2013. Available: https://wwwbrr.cr.usgs.gov/gstl/kinzel_papers/Kinzel_JAWRA_2013.pdf

[4] Sandfort, T., et al., "Bathymetric Structure from Motion," *Remote Sensing*, 2016. Available: https://www.researchgate.net/publication/308765034_Bathymetric_Structure_from_Motion_Extracting_shallow_stream_bathymetry_from_multi-view_stereo_photogrammetry

[5] NOAA, "Lidar Geodesy and Bathymetry," 2020. Available: https://oceanservice.noaa.gov/geodesy/lidar.html

[6] Konda, A., et al., "Materials for Respiratory Masks in the Context of COVID-19 Pandemic," 2020. Available: https://www.researchgate.net/publication/348282324_Materials_for_Respiratory_Masks_in_the_Context_of_COVID_19_Pandemic

[7] Egismos, "Laser Distance Measurer Module M2," 2022. Available: https://www.egismos.com/intergrated-photonics-modules/Laser-distance-measurer-module-M2.pdf

[8] MaxBotix, "MB7388 Ultrasonic Sensor," 2023. Available: https://maxbotix.com/products/mb7388

[9] Adafruit, "Product 4097," 2022. Available: https://www.adafruit.com/product/4097

[10] NXP Semiconductors, "AN3461 Application Note," 2019. Available: https://www.nxp.com/docs/en/application-note/AN3461.pdf

[11] PJRC, "Teensy 4.1 Microcontroller," 2023. Available: https://www.pjrc.com/store/teensy41.html

[12] Hitec RCD, "D646WP 32-bit Digital High Torque Waterproof Servo," 2020. Available: https://hitecrcd.com/d646wp-32bit-digital-high-torque-waterproof-servo/

[13] World Health Organization, "Materials for Respiratory Masks," WHO-FWC-WSH-17.01, 2020. Available: https://www.who.int/publications/i/item/WHO-FWC-WSH-17.01

[14] Southern States, "Hi-Yield Horticultural Hydrated Lime," 2021. Available: https://southernstates.com/products/hi-yield-horticultural-hydrated-lime

[15] YSI Inc., "EXO2 Multiparameter Sonde," 2022. Available: https://www.ysi.com/exo2

[16] USGS, "Turbidity and Water," 2021. Available: https://www.usgs.gov/special-topics/water-science-school/science/turbidity-and-water